SYNTHESIS OF TITANIUM DIOXIDE HETERO-STRUCTURES FOR PHOTOVOLTAIC ENERGY CONVERSION

A Thesis

by

JONGBOK PARK

Submitted to the Office of Graduate Studies of
Texas A&M University
in partial fulfillment of the requirements for the degree of

MASTER OF SCIENCE

August 2009

Major Subject: Mechanical Engineering

SYNTHESIS OF TITANIUM DIOXIDE HETERO-STRUCTURES FOR PHOTOVOLTAIC ENERGY CONVERSION

A Thesis

by

JONGBOK PARK

Submitted to the Office of Graduate Studies of
Texas A&M University
in partial fulfillment of the requirements for the degree of

MASTER OF SCIENCE

Approved by:

Chair of Committee,	Choongho Yu
Committee Members,	Hae-Kwon Jeong
	Xinghang Zhang
Head of Department,	Dennis L. O'Neal

August 2009

Major Subject: Mechanical Engineering

ABSTRACT

Synthesis of Titanium Dioxide Hetero-Structures

for Photovoltaic Energy Conversion. (August 2009)

Jongbok Park, B.S., Korea Military Academy

Chair of Advisory Committee: Dr. Choongho Yu

The photovoltaic energy conversion system (PV cells or solar cells) has been researched over the last few decades, and new technologies have been proposed. At the same time, the synthesis of nano-scale materials has been investigated intensively from the 1990s. These new types of materials encourage the development of new PV technologies with extensive research. Dye-sensitized solar cells (DSSCs) can be a part of these efforts. Since first presented in 1991, DSSCs have become the center of attention due to their great advantages to the traditional silicon solar cells. However, it remains a challenge to develop better performing DSSCs since the efficiency of DSSCs is still much lower than that of high performance solar cells. To meet this challenge, the different types of TiO_2 nanostructures in DSSCs have been studied.

This thesis presents the synthesis of TiO_2 hetero-structures. These structures can achieve two important factors in DSSCs. One is the electron pathway for high electron transport rate, and the other is the large surface area for the dye absorption.

TiO_2 hetero-structures were successfully synthesized by using a simple thermal annealing method. The synthesis method required neither a high reaction temperature

nor complicated reaction processes and produced dense TiO_2 nanowires and incorporating TiO_2 nanoparticles with relatively short reaction time. The key parameters of growing 1-D TiO_2 nanostructures were the Cu eutectic catalyst, the reaction temperatures, and the annealing time. The repetition time and the reaction temperatures were important factors for incorporating TiO_2 nanoparticles.

The structure and composition of as-grown samples were analyzed using an x-ray diffractometer, a scanning electron microscope, a field emission scanning electron microscope, a transmission electron microscope and an ultraviolet-visible spectroscopy. The results showed they were crystalline structures in rutile phase of TiO_2.

From this research, we can utilize hetero-structures as an electrode of DSSCs. We also expect that our simple and effective synthesis method can be used for growing other kinds of metal oxide nanostructures, especially for those melting temperature are high.

DEDICATION

To my lovely wife Eunei, daughter Jimin, my family
&
God

ACKNOWLEDGEMENTS

First of all, I really would like to acknowledge my advisor, Dr. Choongho Yu, for his guidance and support throughout the entire period of my research. I also thank to my committee members, Dr. Hae-kwon Jeong, and Dr. Xinghang Zhang, for their advice and encouragement.

Thank also goes to my wise and lovely wife Eunei for her dedication, love, and patience during my studying. She was the only person who supported me, trusted me, and encouraged me when I was undergoing trials and struggling with my experiments.

Friends made my time at Texas A&M University a great experience. I will not be able to forget them and all the times spent with them at TAMU and College Station. At the same time, I would like to thank to my colleagues, Hongjoo Yang, Liang Yin, Yunki Gwak, Vinay Narayanunni and Marion Okoth, in the Nano-Energy Laboratory. Because of their supports, I could overcome difficult situations during my research. I am also very grateful to Dr. Hansoo Kim for TEM analysis of my samples.

Finally, I want to extend my gratitude to the Republic of Korea Army for the financial support.

TABLE OF CONTENTS

LIST OF FIGURES

LIST OF TABLES

1. INTRODUCTION*

1.1 Motivation

Currently, 80% of the total energy consumption relies on fossil fuels. The increment of worldwide energy demand will reach about 70% between 2000 and 2030. The problem is that fossil fuels are facing rapid exhaustion and causing environmental pollution [1]. Under these circumstances, a new energy technology, which is environmentally friendly and has the competitive energy efficiency, is needed in order to substitute for fossil fuels in the near future. Among new technologies, the photovoltaic energy conversion system is one of the most promising methods. The photovoltaic energy conversion system (PV cells or solar cells) has been researched over last few decades, and new concepts and technologies have been proposed and discovered by various approaching methods. The energy supplied from the sun to the earth is 3×10^{24} J/year which is almost 10,000 times larger than the consumption of the global energy. Simply speaking, if we cover 1/1000 of the earth with solar cells with 10% efficiency, we can satisfy the world energy consumption [2].

In 1954, the first practical conversion of solar radiation into electric energy was demonstrated by using of a p–n junction type of solar cell with 6% efficiency [3]. The silicon photovoltaic cells rapidly became a power source for satellites with the development of the space project. Unfortunately, the widespread use of these silicon solar cells has been prevented due to their relatively high manufacturing cost and

---

This thesis follows the style of *Nanotechnology*.

*Parts of this section reprinted with permission from "Simple and fast annealing synthesis of titanium dioxide nanostructures and morphology transformation during annealing processes" by Jongbok Park, Yeontack Ryu, Hansoo Kim, Choongho Yu, 2009, Nanotechnology, 20, 105608, Copyright [2009] by IOP.

the toxic chemicals produced from the manufacturing process [4]. These matters drove researchers into the field for developing environmentally friendly and low production cost alternatives.

As a result of these efforts, dye-sensitized solar cells (DSSCs) have been presented as promising candidates due to their potential for large scale manufacturing with a low cost. Since the first time presented by O'Regan and Grätzel in 1991, DSSCs have become the center of attention due to their great attraction to the conventional silicon solar cells [5]. Furthermore, DSSCs offer a suitable energy conversion efficiency, up to 11.1% at the condition of air mass(AM) 1.5 full sunlight intensity (1000W/m^2) [6]. This value is comparable to the efficiency of amorphous silicon solar cells. The main difference between DSSCs and conventional silicon solar cells is that DSSCs separates light absorption from charge carrier transport. This kind of a systemic difference means that DSSCs can be composed by lowering the manufacturing cost [5]. In addition, non-toxic materials are used in manufacturing processes which is environmentally friendly.

Traditionally, DSSCs consist of crystalline TiO_2 nanoparticles between two adjacent transparent conducting oxide (TCO) glasses. Nanoparticles were deposited on the TCO and sintered at a moderate temperature to build a continuous network for electron transport. Subsequently, a monolayer of dyes is coated onto this TiO_2 film, and electrolytes are injected between TCO substrates. The solar cell, therefore, is formed into a thin film shape in several micrometers thick.

The mechanism of DSSCs is also simple as shown in figure 1 [7]. The photo-excited dye molecule ejects the electrons to the conduction band of TiO_2 during the

illumination of the cell, and then the electrons travel along this conduction band. Subsequently, those electrons are transferred to the TCO, current collector, and from there they pass through the external circuit performing electrical work. The dye is restored to the original state by the electron donation from the I^-/I_3^- electrolyte reaction which continues the energy conversion cycle.

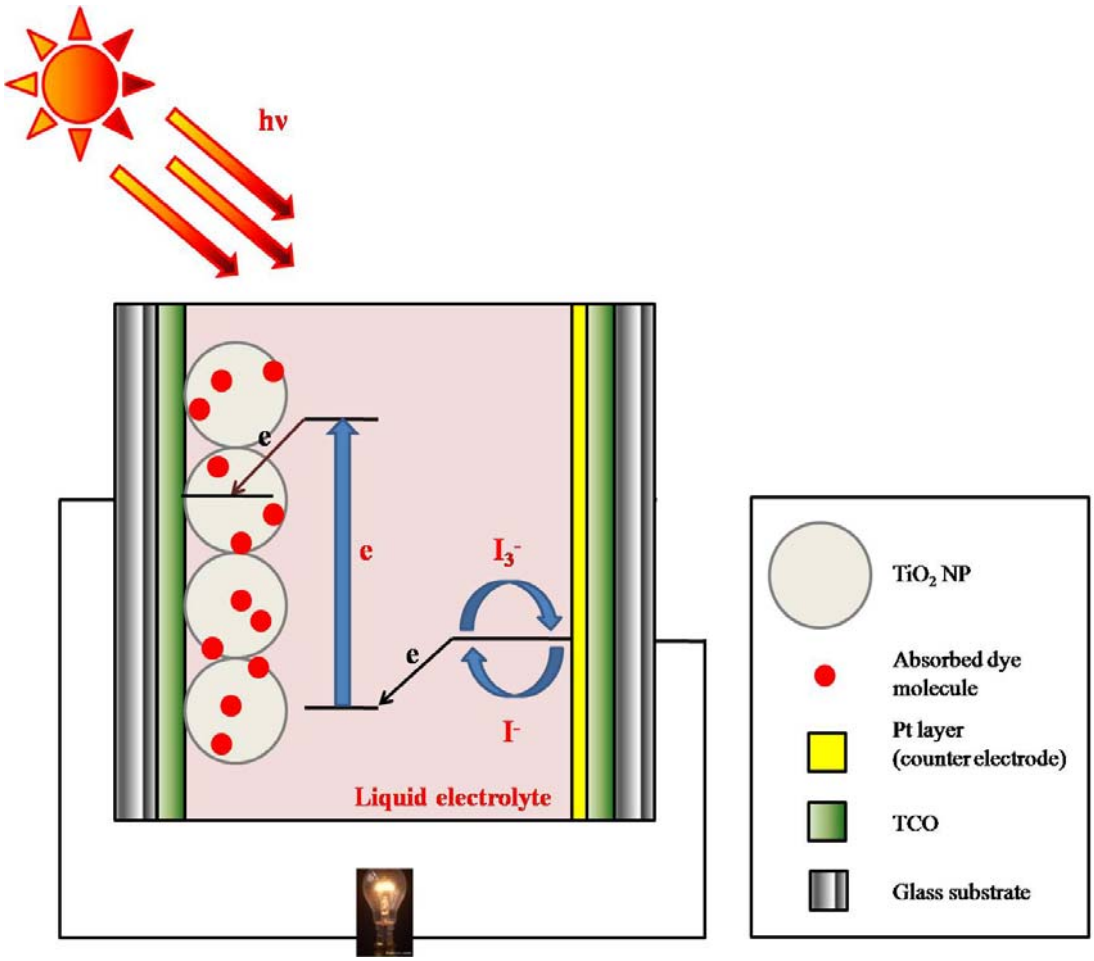

Figure 1. Schematic mechanism of dye-sensitized solar cells.

We should consider the transmittance and the conductivity of the TCO substrate [8, 9], the properties of TiO_2 structures [10-14] and electrolytes [15-17], and the types of dyes [18, 19], all as important factors which affect on the cell performance in energy conversion efficiency. Among these factors, the structural property of TiO_2 is vigorously investigated to demonstrate the influence of the thin layer structure. Up to now, the most common structure for DSSCs is a porous thin film composed of TiO_2 nanoparticles [5, 20]. There are limitations for these types of DSSCs. The electron recombination with oxidized dyes should be much slower than the electron diffusion to guarantee the efficiency. However, the speed of the electron diffusion through the junctions of TiO_2 nanoparticles is several orders of magnitude smaller than the bulk single crystal TiO_2 due to electron traps and boundaries at the junctions of nanoparticles [21-25].

Therefore, new types of thin layer structures are needed to make up for the weak point of the DSSCs composed of only nanoparticles. To satisfy this need, many researchers have suggested the thin layer which is composed of one-dimensional TiO_2 nanostructures as new candidates. Actually, there is a report that DSSCs which consist of fully crystalline TiO_2 nanotube array films demonstrate much slower recombination than the nanoparticle-based DSSCs [26]. One-dimensional (1-D) TiO_2 nanostructures optimize the conduction pathway to eliminate recombination of the charge carriers by transferring the electrons as quickly as possible which is a crucial factor in cell performance [27, 28]. In other words, all the electrons injected from the photo-excited dye into the TiO_2 conduction band are easily transported to the current collector along 1-

D nanostructures [29]. Furthermore, these kinds of nanostructures can also scatter light and this effect causes the augmentation of the light harvesting [12].

Nevertheless, the only reason why 1-D nanostructures of DSSCs cannot beat the performance of nanoparticle-based DSSCs is the smaller surface area for the dye absorption than nanoparticle-based DSSCs. To better this kind of problem, the method of incorporating nanoparticles into nanowires have been suggested, recently [12, 14]. By utilizing this type of film for DSSCs, the enhancement of the light harvesting and the increase of the electron transport rate can be achieved by the part of nanowires structure. At the same time, the incorporating nanoparticles can provide a large surface area to maximize the dye absorption. There is a report that the energy conversion efficiency was enhanced by using this kind of a thin layer [12]. However, the junctions still remains as a problem because the nanoparticles and nanowires were sintered after mixing together. Therefore, the new synthesis approach is needed in order to improve the junctions between nanoparticles and nanowires.

1.2 Literature Review

One-dimensional nanostructure forms such as nanowires, nanotubes, and nanobelts have been preferred as they often bring performance enhancement for various applications including the example mentioned in a previous section [28, 30-32]. Thus, many researchers have invested a great deal of effort in the synthesis of 1-D TiO_2 nanostructures [33]. For example, Ti powders were used to deliver Ti on a Au-coated TiO_2/Si substrate so as to produce nanowires whose lengths are up to ~3 μm in a

vacuumed high-temperature tube furnace [34]. Similar synthesis methods that employ a vacuumed reaction chamber have been popular for growing a few micron long nanowires [35, 36] unless the nanowire growth occurs in a liquid environment. The vacuumed environment often impedes the formation of film-like titanium oxides that often hinder titanium nucleations for directional growths due to their high stability and high melting temperature (~1870 °C). Other methods include a sol-gel method with anodic alumina membranes [37], a hydrothermal synthesis in high concentration of NaOH or dilute HNO_3 [38], a reaction between the layered compound $Na_2Ti_3O_7$ particles and the dilute HCl in an autoclave for several days [39], and a fabrication method for obtaining nanowire arrays from UV photolithography and subsequent dry-etching of TiO_2 thin films [40]. These methods often require various chemical reagents, multiple processes with relatively long reaction time, careful time-consuming sample preparations, or expensive equipment. For instance, template-based synthesis methods using porous alumina membranes require time-consuming and cumbersome processes for membrane fabrications [41-43]. Moreover, it is very inconvenient to separate nanomaterials from the membrane as this requires extra steps for dissolving alumina and subsequent centrifuge processes.

1.3 Objectives

This thesis presents a simple and fast approach of synthesizing 1-D TiO_2 nanostructures and TiO_2 nanoparticles for the DSSCs applications. The synthesis method of 1-D TiO_2 nanostructures produced relatively long (~10 μm) nanowires with

only ~30 minutes reaction time and longer nanostructures up to ~30 μm with 2~4 hour reaction time at temperatures much lower than the melting point of Ti. Furthermore, morphology changes from wire to belt-like shapes have been observed by extending the reaction time.

The direct incorporation method of TiO_2 nanoparticles with TiO_2 nanowires was also investigated for synthesizing TiO_2 hetero-structures. The nanoparticles were directly incorporated on the pre-grown nanowires structure by using repeated thermal annealing processes. The purpose of direct incorporation of TiO_2 nanoparticles is to obtain better contacts between nanoparticles and nanowires. By applying the thin layer of this nanostructure to the DSSCs as an electrode, the junction problem between nanoparticles and nanowires caused by the conventional sintering process can be improved while the advantages of both structures are maintained. The scheme of the proposed TiO_2 hetero-structure is depicted in figure 2.

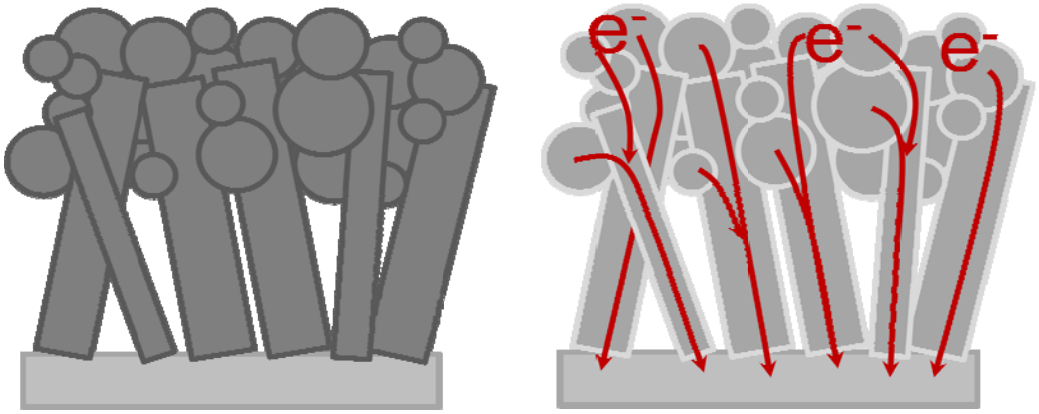

Figure 2. Scheme of proposed TiO_2 hetero-structures for DSSCs.

Moreover, this method does not need an ultra high reaction temperature, sophisticated processes, expensive apparatus, a long reaction time, and a vacuum system. Particularly, this simple synthesis process has not been addressed in the past due to the high melting point (~1668 °C) and strong oxygen affinity of Ti although simple annealing processes have recently been adopted for growing several metal-oxide nanostructures using low-melting point metals such as Zn, Sn, Mg, In, and Ga [44, 45]. The following sections describe detail experimental conditions and key parameters, including annealing temperatures, reaction time, a catalyst and also present structures and morphologies of as-grown TiO_2 nanostructures.

2. SYNTHESIS OF 1-D TiO_2 NANOSTRUCTURES*

2.1 Experimental Details

Titanium foils (Sigma-Aldrich, purity 99.7 %) were diced into pieces (~0.5 cm × 0.5 cm × 0.1 mm), and then ultrasonically cleaned in acetone, isopropanol, and deionized (DI) water, respectively. A catalyst solution was prepared by dissolving $CuCl_2 \cdot 2H_2O$ (Acros Organics, purity 99 %) in DI water with a concentration of 0.005M. Then, the solution was spin-coated three times at 1500 rpm for 20 seconds. The spin-coating process uniformly distributes tiny $CuCl_2$ particles on the foil surface, and makes it possible to use a relatively low reaction temperature due to the low Ti-Cu eutectic temperature (~870 °C) compared to the Ti melting point [46]. Upon heating, $CuCl_2$ decomposes into CuCl and gas-phase Cl_2 above 493°C (i.e., $CuCl_2$ (s) → CuCl (s/l) + 0.5 Cl_2 (g)) [47]. CuCl reacts with Ti even at low temperature (~250 °C), remaining only solid Cu, (i.e., Ti (s) + 4CuCl (s) → $TiCl_4$ (g) + 4Cu (s)) [48, 49]. Consequently, this results in uniform Cu particle depositions as the gas-phase $TiCl_4$ moves away from reaction sites in Ar flow during reaction processes. The sample was placed in a covered boat that prevents Cu from being lost to the Ar flow and was inserted at the center of a quartz tube of ~120 cm in length and ~2.3 cm in inner diameter as shown in figure 3. The boat has an opening on the side where a slow Ar flow impinges during synthesis processes. Both ends of the tube were sealed by O-rings and end caps. Prior to heating the tube furnace, ~100 sccm Ar was flowed for 3 minutes in order to remove air or any residues that might be present in the tube. Subsequently, the furnace was heated up to

*This section reprinted with permission from "Simple and fast annealing synthesis of titanium dioxide nanostructures and morphology transformation during annealing processes" by Jongbok Park, Yeontack Ryu, Hansoo Kim, Choongho Yu, 2009, Nanotechnology, 20, 105608, Copyright [2009] by IOP.

the growth temperatures (see table 1) with a continuous ~40 sccm Ar flow throughout the entire synthesis process.

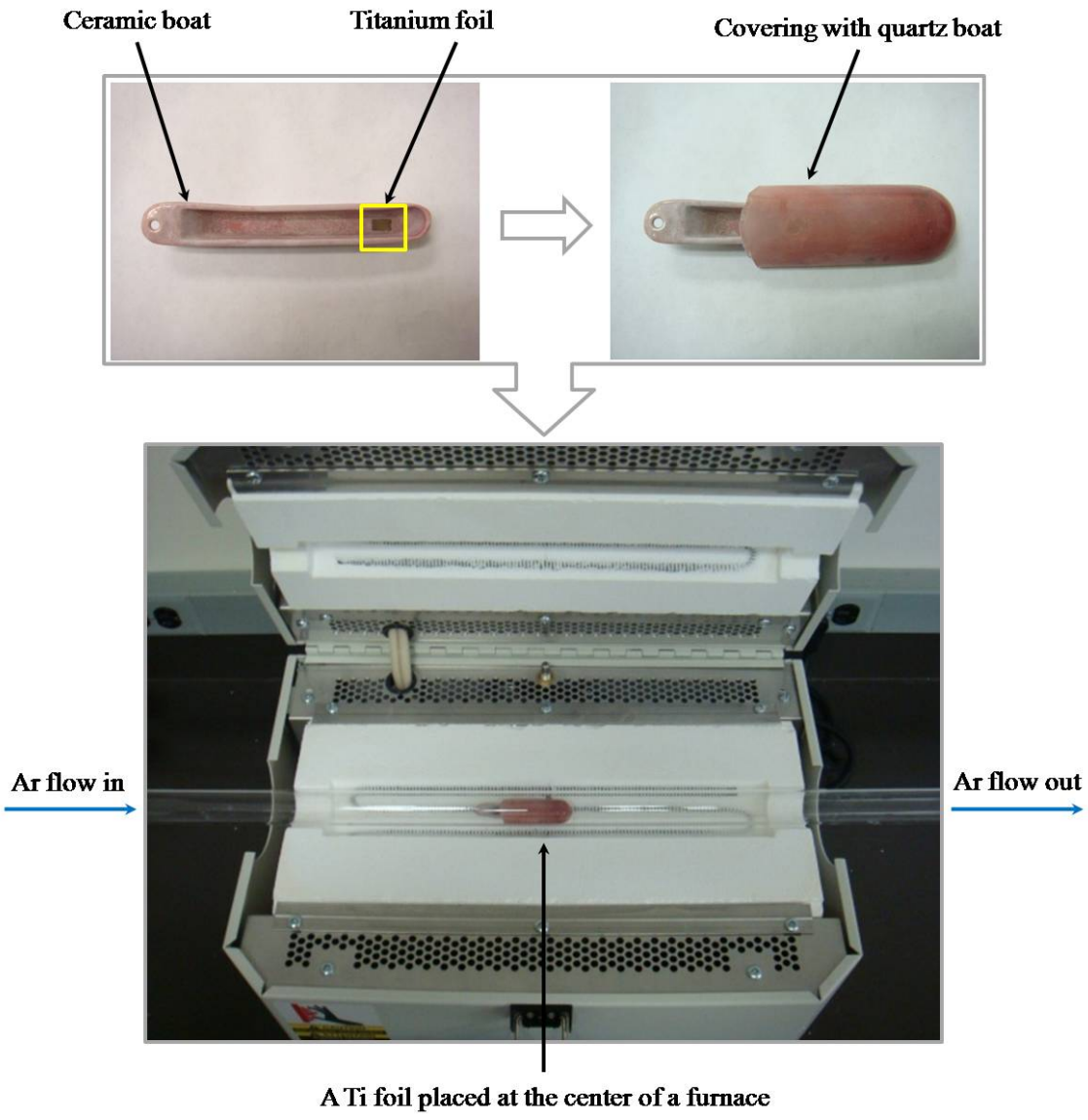

Figure 3. Experimental setup to synthesize 1-D TiO_2 nanostructures.

Table 1. Nine different 1-D nanostructures synthesis conditions. One parameter was changed at a time from the condition 1 to 7, and the condition 8 is to compare the results with the condition 1 and 2. The condition 9 is to find the influence of oxygen contents on the nanostructure growth during the reaction. Cu was used as a eutectic catalyst for all reactions except for the synthesis condition 5.

Synthesis condition	**Annealing Temperature (°C)**	**Annealing time (min)**	**Ramping time (min)**	**Remark**
1	750	30	20	
2	850	30	20	
3	850	30	85	
4	850	120	85	
5	850	120	85	Annealed without Cu
6	850	240	85	
7	850	360	85	
8	950	30	20	
9	850	30	20	Annealed in room air

Nine different synthesis conditions were tested as listed in table 1 for elucidating the influence of three important synthesis parameters, growth temperatures, annealing time, and seed catalyst, on nanostructure growth and morphology. Three different annealing temperatures, 750 °C, 850 °C, and 950 °C were used. These temperatures – close to the eutectic temperature, ~100 °C lower or higher than the eutectic temperature – were selected so as to find the influence of the catalyst. In other words, the nanowire growth would be the most vigorous at a temperature close to the eutectic temperature if the catalyst plays a significant role in the synthesis. Two different ramping times were used to find the response of slow and fast temperature changes, and four different annealing times were employed in order to identify any changes in nanowire morphologies. At the end of the annealing, the furnace temperature was set to a room temperature for fast cooling, but it was cooled naturally due to no active cooling equipment attached to the furnace. The cooling rate was approximately 10 °C/min above ~200 °C and approximately 1 °C/min below ~200 °C.

The structure and composition of as-grown samples were analyzed by using an X-ray diffractometer (Bruker-AXS D8 VARIO), a scanning electron microscope (SEM, JEOL JSM-6400), and a field emission scanning microscope (FE-SEM, FEI Quanta 600). For the X-ray diffraction (XRD) analysis, nanostructures prepared by using the synthesis condition 4 in table 1 were ultrasonically detached from the foil in deionized water. Then, the sample-containing solution was dispersed and dried on a quartz substrate several times. The sample was scanned from $2\theta = 20°$ to 60° with a step size and dwell time of 0.01° and 0.1 second, respectively. In addition, they were also used for more

detailed analysis in a transmission electron microscope (TEM, JEOL JEM-2010). The nanostructures were detached by sonication in deionized water, and then they were dispersed on a thin pure formvar resin coated meshed grids. High-resolution and selected area electron diffraction (SAED) images were also presented.

2.2 Results and Discussion

1-D TiO_2 nanostructures were successfully obtained as shown in figures 4(a), (b), (c), (d), and (f) with the growth conditions, 1, 2, 3, 4, and 6 in table 1, respectively. The influence of the reaction temperature was studied by comparing the morphology of nanowires in figures 4(a), (b) and (h), whose reaction temperatures were 750 °C (condition 1), 850 °C (condition 2), and 950 °C (condition 8), respectively. The nanostructures grown at 750 °C were relatively short (~5 μm long) and thin (typically smaller than 100 nm in diameter). The density of wires was lower than that of wires grown at the 850 °C reaction temperature, which produced ~10 μm long and ~100 nm in diameter nanowires with the same reaction time. When we increased the annealing temperature to 950 °C, however, most of nanostructures were short, thick, and rod-shaped. The optimum growth temperature close to Ti-Cu eutectic temperature indicates that the Cu catalyst plays a major role in the growth of the nanostructures. Furthermore, without using the catalyst, no nanostructures were obtained, as shown in figure 4(e), by using simple annealing methods employed for synthesizing other nanostructures [50-52].

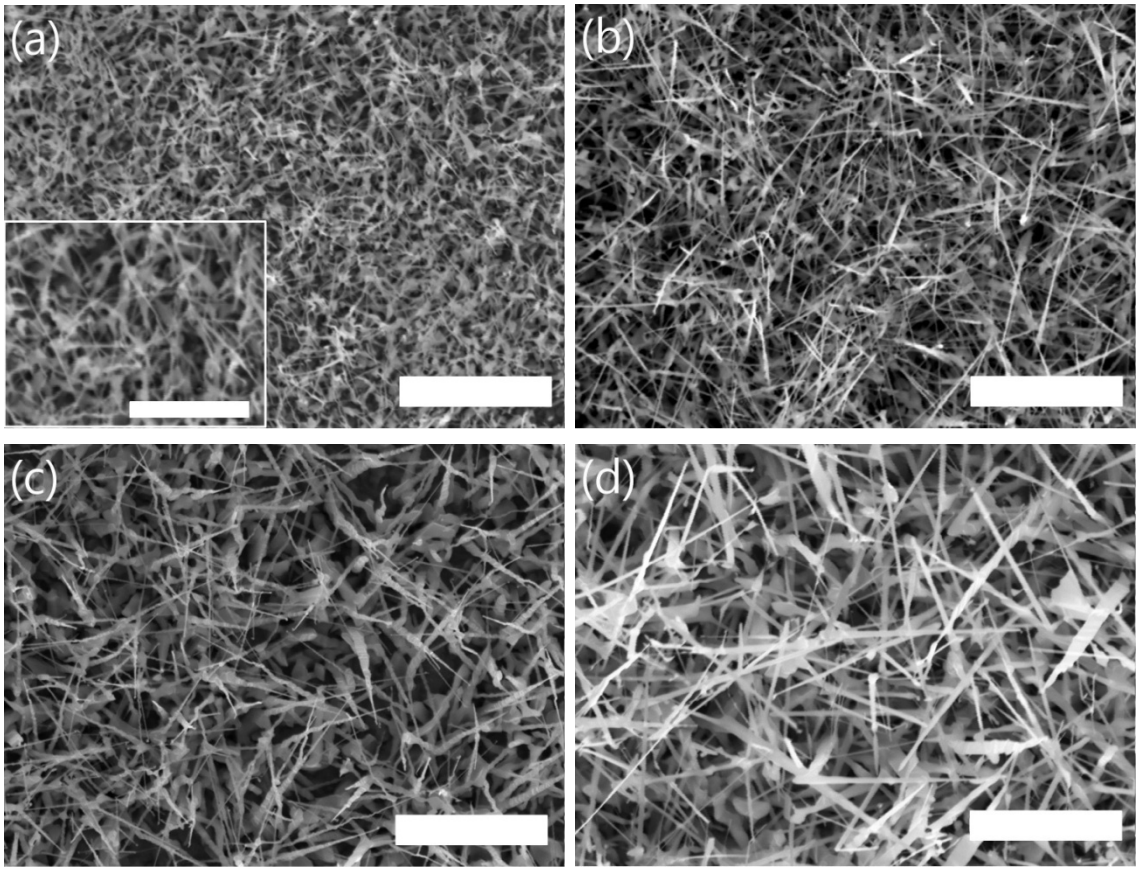

Figure 4. SEM images of 1-D TiO_2 nanostructures grown by using different growth conditions as listed in table 1. (a) 20 min ramping/30 min annealing at 750 °C (condition 1), (b) 20 min ramping/30 min annealing at 850 °C (condition 2), (c) 85 min ramping/30 min annealing at 850 °C (condition 3), (d) 85 min ramping/120 min annealing at 850 °C (condition 4), (e) 85 min ramping/120 min annealing at 850 °C without incorporating Cu catalysts (condition 5), (f) 85 min ramping/240 min annealing at 850 °C (condition 6), (g) 85 min ramping/360 min annealing at 850 °C (condition 7), (h) 20 min ramping/30 min annealing at 950 °C (condition 8), (i) 10 min ramping from ~23 °C to 650-670 °C, followed by an immediate natural cooling at ~23 °C. The scale bars in the inset of (a) and (i) represent 5 μm and 500 nm, respectively. All other scale bars indicate 10 μm.

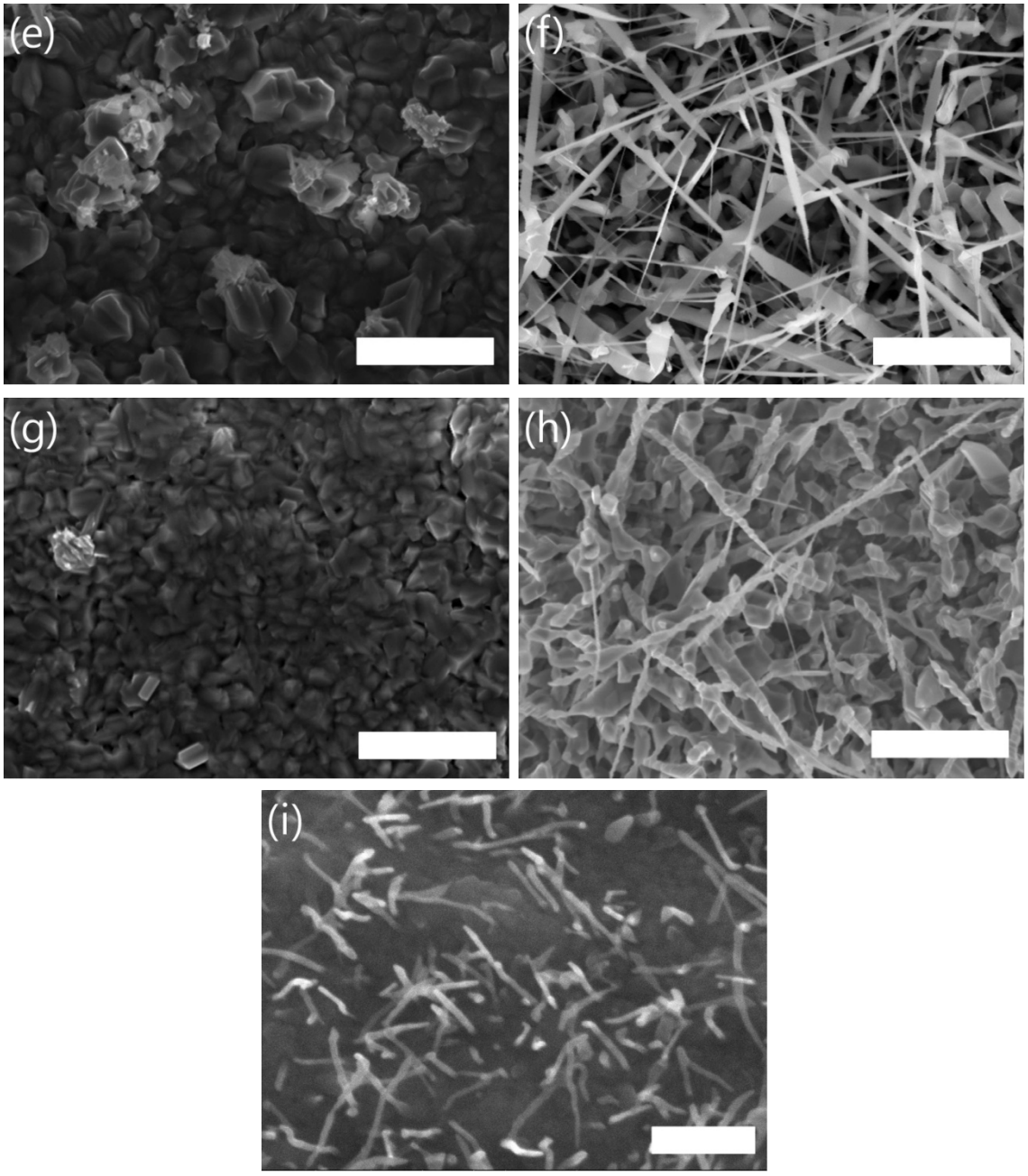

Figure 4. Continued.

So far, various growth mechanisms of metal-oxide nanostructures have been proposed such as vapor-liquid-solid (VLS) [53], vapor-solid (VS) [54], and solid-liquid-solid (SLS) [55] growth processes. The VLS mechanism is common for catalyst-assisted nanowire syntheses, but catalyst particles were not easily observed at the end of the nanowires in this study. Hence, this method is thought to be rather close to solid-liquid-solid or/and solid/vapor-liquid/solid phase reactions, but it would be different from spontaneous growth mechanisms that have been reported in the past [44, 50, 56, 57].

A proposed growth reaction in this study is the following as schematically shown in figure 5. First, a thin layer of Ti reacted with Cu catalysts creating liquid-phase islands or Ti-Cu interfaces, which were served as seeds for slender nanostructures (figure 5(a)). Oxygen was easily diffused into the liquid phase Ti, producing crystalline TiO_2. In addition, Ti particles can be delivered to the seeds by diffusion or/and vapor (figure 5(b)). The nanowire growth in the axial direction requires Ti to be delivered from the surface of the foil. As they become longer, less Ti can be delivered to their tips. This often promotes lateral and new growths, resulting in tapered & belt-like nanostructures shown in figure 4. At the same time, oxygen easily diffuses into Ti foil surfaces at high temperature, producing oxide layers, due to the strong oxygen affinity of Ti. A merger of the nanowires/belts also occurs due to the high density and lateral growth of the nanostructures (figure 5(c)). Longer reaction at high temperature buries nanostructures owing to the slow growth in the axial direction compared to the surface oxidation and lateral growth (figure 5(d)).

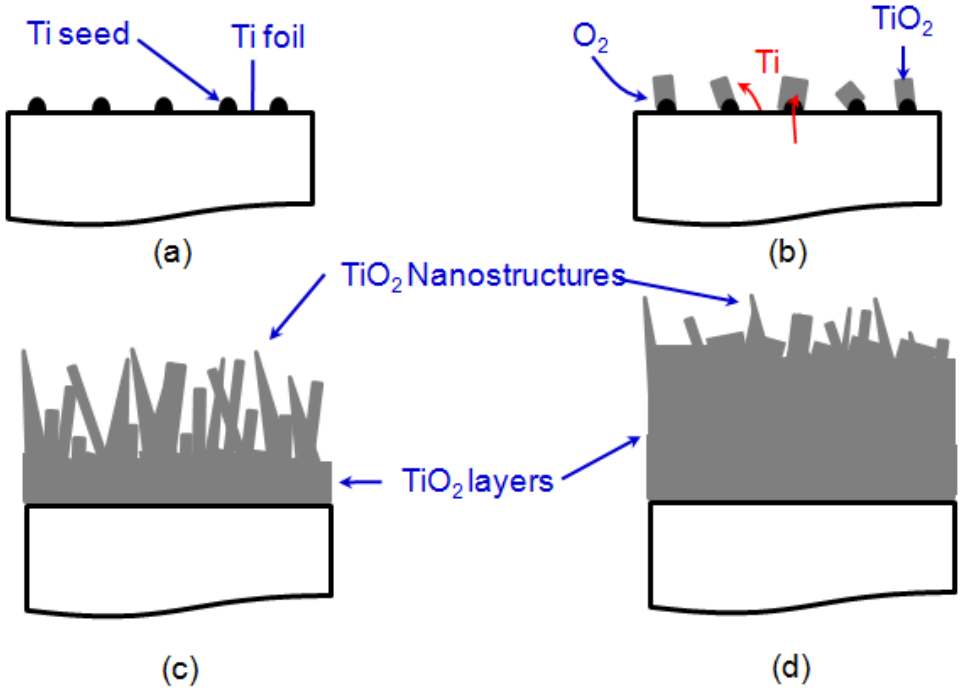

Figure 5. Proposed 1-D TiO_2 nanostructures growth mechanism. (a) Ti nucleation initiates and liquid phase islands form. (b) Oxygen diffuses into the nucleation sites, producing crystalline TiO_2. Ti is delivered from the surface of the Ti foil. (c) Further reaction produces both axial and lateral growth of the nanostructures and oxidation layers from the surface. (d) A long reaction produces a thick layer of TiO_2 due to the slow reaction of the nanostructures in the axial direction compared to the oxide layer and lateral growths.

In order to elucidate the growth mechanism, we stopped the process at an early growth stage. The furnace temperature was increased for only 10 minutes with the fastest ramping rate (~65 °C/min). When the furnace temperature reached to 650~670 °C, the sample was immediately taken out from the tube furnace. As shown in

the figure 4(i), nucleation sites were found on the foil surface, and many of them became a few hundred nm long nanowires even with such short period reaction time. Note that such nucleation was not observed when the maximum reaction temperature was ~550 °C or lower.

The density of nanostructures was considerably reduced without the boat cover and higher for the sample grown on rough-surface foils than smooth ones. The cover would have increased the Ti-Cu reaction probability and facilitated long nanowire growths with shorter reaction times than those obtained by using other approaches [50-52, 58-63]. The rough surface would have promoted the protrusion from the foil surface, which helps the slender structure formation. The 950 °C reaction temperature, which is much higher than the eutectic temperature, would have hindered the formation of isolated nucleation, producing thick-root nanorods as shown in figure 4(h). A long time reaction produced a film-like oxide layer rather than slender nanostructures as shown in figure 4(g). For comparison, the samples grown by synthesis conditions 4 and 7 were cold-fractured using liquid nitrogen in order to inspect their cross sections as shown in figures 6(a) and 6(b). The inset of figure 6(a) shows nanostructures embedded in as well as protruded from the thick oxide layer, but nanowires over the top of the oxide layer are hardly seen in figure 6(b). Only thin oxide layer was observed on the bottom side of the sample grown with the condition 4 while a thick oxide layer was deposited on the bottom of the sample grown with the condition 7.

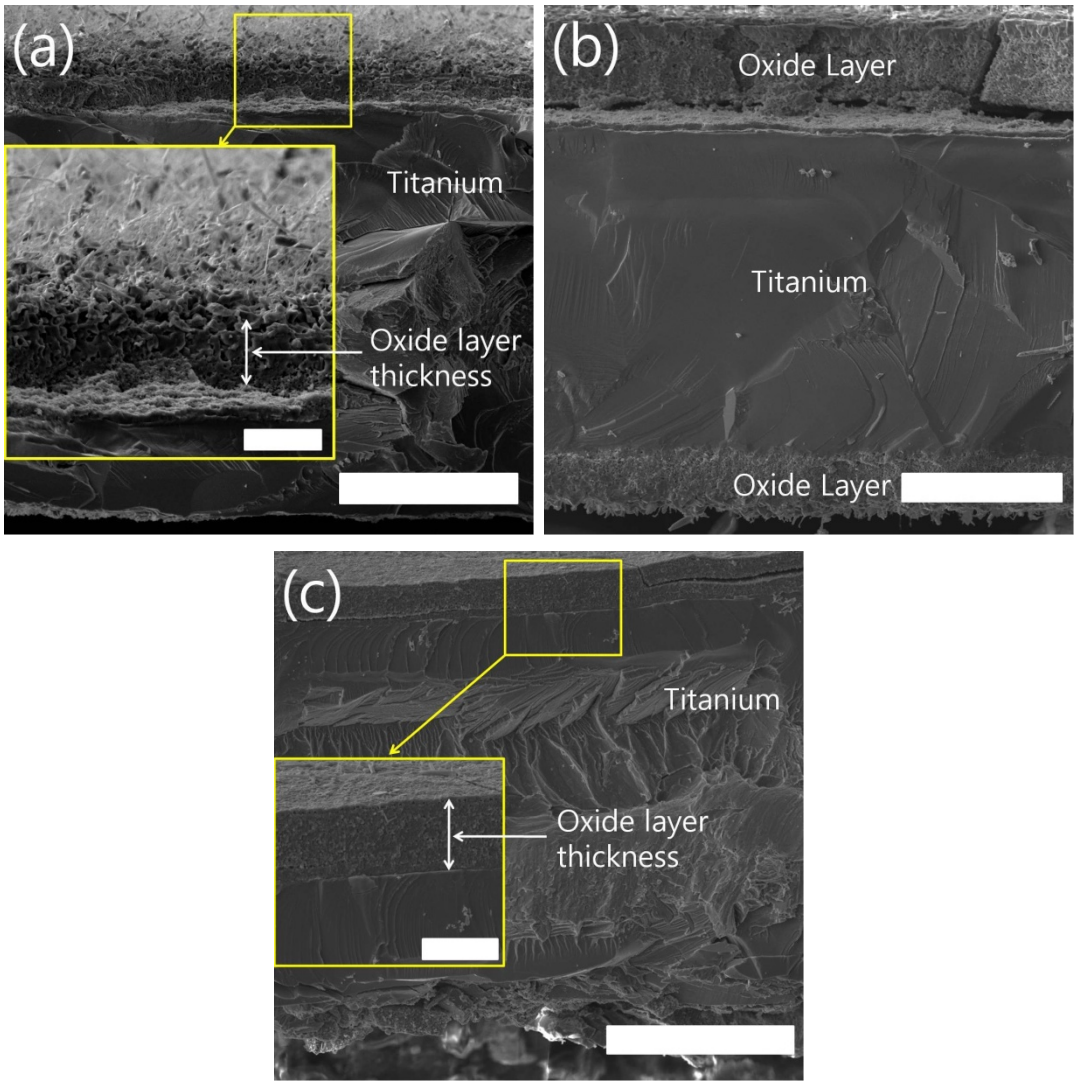

Figure 6. Cross section images of the samples. (a) 85 min ramping / 120 min annealing at 850 °C (condition 4), (b) 85 min ramping / 360 min annealing at 850 °C (condition 7), (c) 20 min ramping / 30 min annealing at 850 °C in room air (condition 9). The insets are enlarged images of the portions enclosed by yellow rectangles. All scale bars other than the one in the inset represent 50 μm, and the scale bar of the inset represents 10 μm.

This indicates that the long reaction results in a thick oxide layer and hampers nanostructure growths. It should be noted that the catalyst solution was not dispersed on the bottom side of the sample. Therefore, only small amount of catalysts would have been delivered to the bottom side. On the other hand, when the foils were annealed in room air, a dense thick oxide film was observed rather than nanostructures (figure 6(c)). We believe that, with a plenty of oxygen in room air, the titanium oxidation process is intense, resulting in such thick oxide layer within a short period of time. This excludes the possibility of so-called hot plate methods in room air, which were employed for growing copper oxide nanostructures [44, 57], for the synthesis of nanostructured TiO_2. In this study, oxygen was not supplied externally to the furnace tube during the reaction, but the oxygen is present from air residues and the Ar gas as impurity (oxygen in the 99.999% pure Ar gas is typically less than ~5 ppm) or/and native oxide layers on the Ti foils. This result suggests that an external supply of oxygen may not be necessary or should be avoided for titanium oxide nanostructure synthesis.

When the annealing time was relatively long, 120 min (condition 4), belt-like nanostructures were appeared (figure 4(d)). Note that they are a mixture of both nanowires and belts. The morphology change was manifested when the annealing time was extended to 240 minutes (condition 6, figure 4(f)). The belt-like structures became very wide (up to ~2 μm) and their lengths were measured to be up to ~30 μm. To our best knowledge, without varying the growth temperature, such morphology changes by simply extending annealing time have not been reported elsewhere. Nevertheless, it would be worthwhile to look into other direct synthesis of belt-like nanomaterials and

infer the factors that determine the shape of nanostructures. For example, MgO nanostructure morphology (nanowires or nanobelts) was determined by their growth temperatures [64]. In this case, the nanostructure growth was governed by VLS mechanisms, which were promoted by Sn particles clearly seen at the end of the nanostructures. At an elevated temperature, the seed particles were merged so as to have slender-shape seeds, resulting in belt-like nanostructures. On the other hand, SnO_2 and Al_2O_3 nanobelts have been obtained without using such eutectic materials required for VLS methods [65, 66]. The preferential growth directions are associated with surface energy and growth kinetics [67]. The growth to the direction normal to the plane with a low surface energy can be suppressed while high energy surface is activated for further reactions. While more extensive study in the future would help to better understand the mechanism that caused the shape change, a preferential growth in the rutile TiO_2 might have brought the morphology changes in this study.

The growth direction of the nanobelts was observed to be <110>, which was confirmed with the lattice fringes and the diffraction spots, as shown in figures 7(a), (b), and (c). The growth direction and structure of nanowires were the same as those of nanobelts as confirmed in figures 7(d), (e), and (f). The high resolution images and the diffraction patterns are aligned along the 001 zone axis of the rutile titania. A rutile structure of TiO_2 is the primitive tetragonal crystal structure with lattice parameters of a = 0.4593 and c = 0.2959 nm (JCPDS file number 21-1276). This growth direction was observed in other study that uses a high temperature (~1050 °C) VLS synthesis [34, 68], while a moderate temperature (~850 °C) annealing method produced nanowires with a

growth direction of <200> [36] and ethanol assisted synthesis method at 750 °C produced <001> [35]. This is a strong indication that nanostructure growths are strongly affected by various parameters including reaction temperature, pressure, and reaction chemistry in addition to the growth kinetics and surface energies. Note that low temperature synthesis methods are not discussed here as they often produced the anatase phase rather than rutile [69-73].

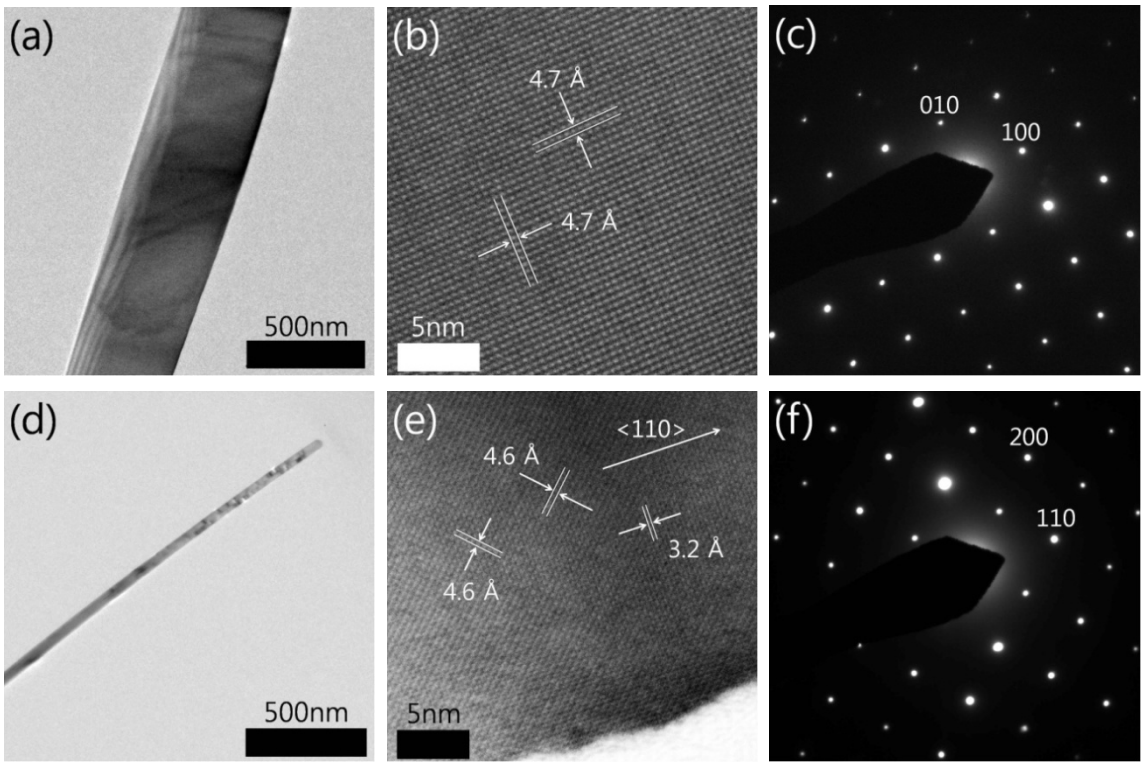

Figure 7. TEM images of 1-D TiO_2 nanostructures. Images of a nanobelt in (a) a low magnification, (b) a high magnification, and (c) a selected area electron diffraction (SAED) pattern of a nanobelt. Images of a nanowire in (d) a low magnification, (e) a high magnification, and (f) a SAED pattern of a nanowire. The sample was prepared at 850 °C with 120 min reaction time (condition 4).

The TiO_2 structures were analyzed by XRD as shown in figure 8, XRD peaks indicate that the nanostructures are in the rutile structure, which is a common and stable form of TiO_2 [34, 35] synthesized at a temperature higher than ~600 °C [73, 74]. Chlorine-containing compounds such as $TiCl_2$, $TiCl_3$, $TiCl_4$, and $CuTiCl_4$ were not detected. In addition, no peaks related to Cu or copper oxides, which may be present as they were used as a eutectic catalyst, were observed. The amount of Cu dispersed on the Ti foil from the low concentration solution may be too small to be detected by the XRD scan.

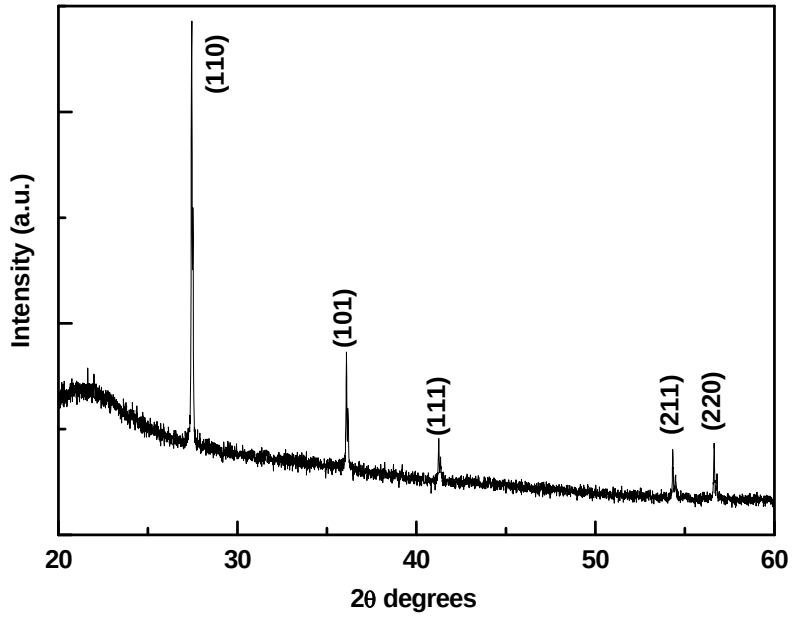

Figure 8. XRD pattern of 1-D TiO_2 nanostructures. The sample was grown at 850 °C with 120 minutes annealing time (condition 4). This result indicates the TiO_2 is in the rutile structure. Crystal directions of the rutile structure TiO_2 are designated in the figure.

3. INCORPORATION OF TiO_2 NANOPARTICLES

3.1 Experimental Details

Titanium powders (Acros Organics, 100mesh, purity 99.7 %) were mixed with $CuCl_2 \cdot 2H_2O$ powders (Acros Organics, purity 99 %) and ground using a mortar. The mixed powders were used in order to develop the gas-phase $TiCl_4$ during the experimental stage. Upon heating, $CuCl_2$ in the mixed powders decomposes into CuCl and gas-phase Cl_2 above 493°C (i.e., $CuCl_2$ (s) → CuCl (s/l) + 0.5 Cl_2 (g)) [47]. CuCl reacts with Ti even at low temperature (~250 °C), remaining only solid Cu, (i.e., Ti (s) + 4CuCl (s) → $TiCl_4$ (g) + 4Cu (s)) [48, 49]. Consequently, the gas-phase $TiCl_4$ is delivered to the sites of TiO_2 nanowires by Ar flow during reaction processes. The delivered $TiCl_4$ gases are used as a seed material to synthesize the TiO_2 nanoparticles.

As a starting structure, TiO_2 nanowires were prepared by using the same procedure mentioned in Section 2.1. The sample and the mixed powders were placed in each side of a covered ceramic boat (2.5 inches long) that maintains $TiCl_4$ gases from being lost to the environment easily, and the boat was inserted at the center of a quartz tube of ~120 cm in length and ~2.3 cm in inner diameter as shown in figure 9. The boat has an opening on the side where a slow Ar flow impinges during synthesis processes. Both ends of the tube were sealed by O-rings and end caps connected with flexible Teflon tube, which can allow the quartz tube to move freely during the annealing processes. Prior to heating the tube, ~40 sccm Ar was flowed for 2 minutes in order to remove air or any residues that might be present in the tube. Subsequently, the tube was

placed in the furnace which is already heated up to the target temperatures (see table 2) with a continuous ~40 sccm Ar flow throughout the entire synthesis process. These processes were repeated as followed by the repeated time conditions listed in table 2, and when the annealing process was repeated, the same amount of the mixed powders was newly loaded.

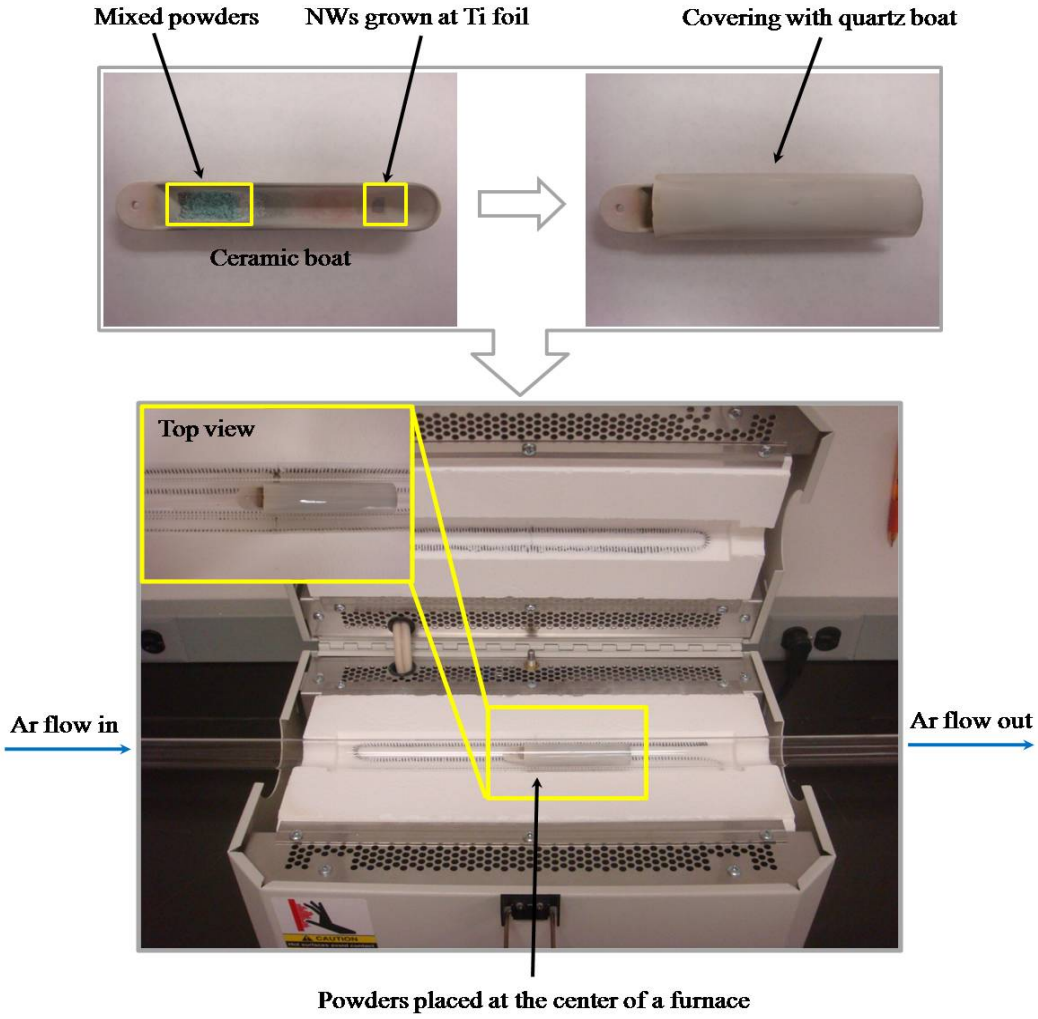

Figure 9. Experimental setup to incorporate TiO_2 nanoparticles.

Table 2. Eight different nanoparticles incorporation conditions. One parameter was changed at a time from the condition 1 to 5, and the condition 6 is to compare the results with the condition 4 by the location of the sample in the furnace. The condition 7, 8 were examined to find the influence of the loading mixed powders from the beginning of the nanowires growth. Condition 3 and 4 are compared to find the influence of the amount of mixed powders.

Synthesis condition	**Incorporating temperature (°C)**	**Initial NWs growth conditions (°C/ min)**	**Repetition time (min)**	**Mixed powders ($Ti/CuCl_2 2H_2O$) (g)**	**Remarks**
1	850	850/30	60/30/30	0.024/0.086	
2	750	850/30	60/30/30	0.024/0.086	
3	750	850/30	20/20/20/20	0.024/0.086	
4	750	850/30	20/20/20/20	0.012/0.043	
5	650	850/30	20/20/20/20	0.012/0.043	
6	750	850/30	20/20/20/20	0.012/0.043	Place to downstream
7	850	-	30/20/20/20	0.024/0.086	Simultaneous process
8	750	-	30/20/20/20	0.024/0.086	Simultaneous process

Eight different synthesis conditions were carried out as listed in table 2 for elucidating the influence of three incorporating parameters, reaction temperatures, the repetition time, and the amount of mixed powders. Three different annealing temperatures, 650 °C, 750 °C, 850 °C, and three different repetition times were employed in order to identify any changes in the size and the density of nanoparticles. Especially, the condition 5 and 6 were examined for the purpose of protecting nanowires from being destroyed by repeated annealing processes as introducing a comparatively lower reaction temperature. In case of the condition 6, the sample was placed downstream and shifted 2.5 inches from the furnace center. By doing this, the mixed powders remain in the active heating area while the sudden temperature drop occurs at the site of the sample. In order to anneal the samples only during the exact repetition time in the condition table, the quartz tube was placed and removed from the furnace at the targeted annealing temperature and cooled down rapidly at a room temperature right after annealing.

The structure and composition of as-grown samples were analyzed by using an X-ray diffractometer (Bruker-AXS D8 VARIO), a field emission scanning electron microscope (FE-SEM, FEI Quanta 600). For the X-ray diffraction (XRD) analysis, nanostructures prepared by using the synthesis condition 4 in table 2. The sample was scanned from $2\theta = 20°$ to 60° with a step size and dwell time of 0.01° and 0.5 second, respectively. In addition, they were also used for more detailed analysis in a transmission electron microscope (TEM, JEOL JEM-2010). The nanostructures were detached by sonication in deionized water, and then they were dispersed on a thin pure

formvar resin coated meshed grids. High-resolution and selected area electron diffraction (SAED) images were also presented.

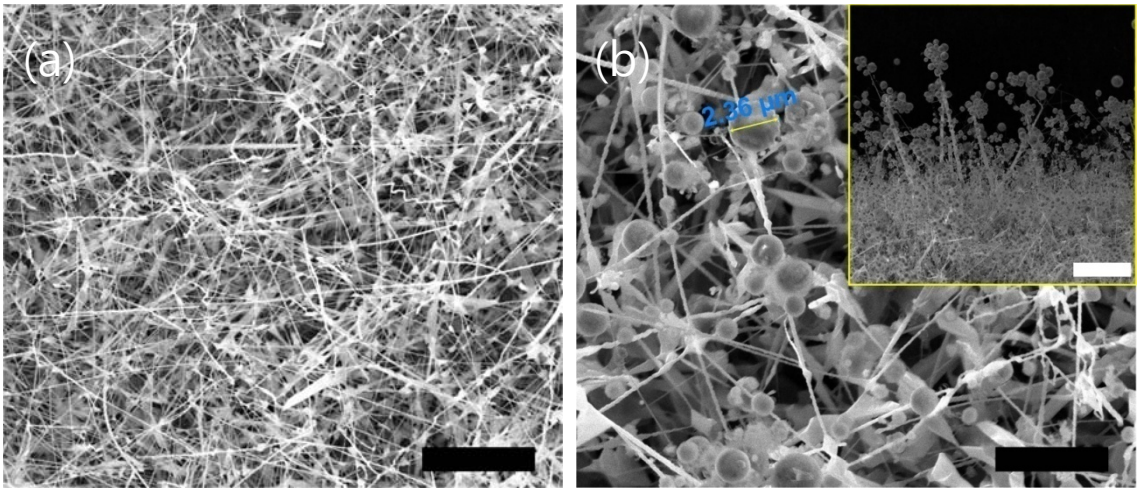

Figure 10. FE-SEM images of TiO_2 hetero-structures grown by using different growth conditions as listed in table 2. (a) An initial nanowires structure (30 min annealing at 850 °C), (b) 60/30/30min annealing at 850 °C (condition 1), (c) 60/30/30min annealing at 750 °C (condition 2), (d) 20/20/20/20min annealing at 750 °C (condition 3), (e) 20/20/20/20min annealing at 750 °C with reduced mixed powders (condition 4), (f) 20/20/20/20min annealing at 650 °C (condition 5), (g) 20/20/20/20min annealing at 750 °C/ placed to downstream (condition 6), (h) 30/20/20/20min annealing at 850 °C by simultaneous process (condition 7), (i) 30/20/20/20min annealing at 750 °C by simultaneous process (condition 8). The scale bars in the insets represent 20 μm, and all other scale bars indicate 5 μm.

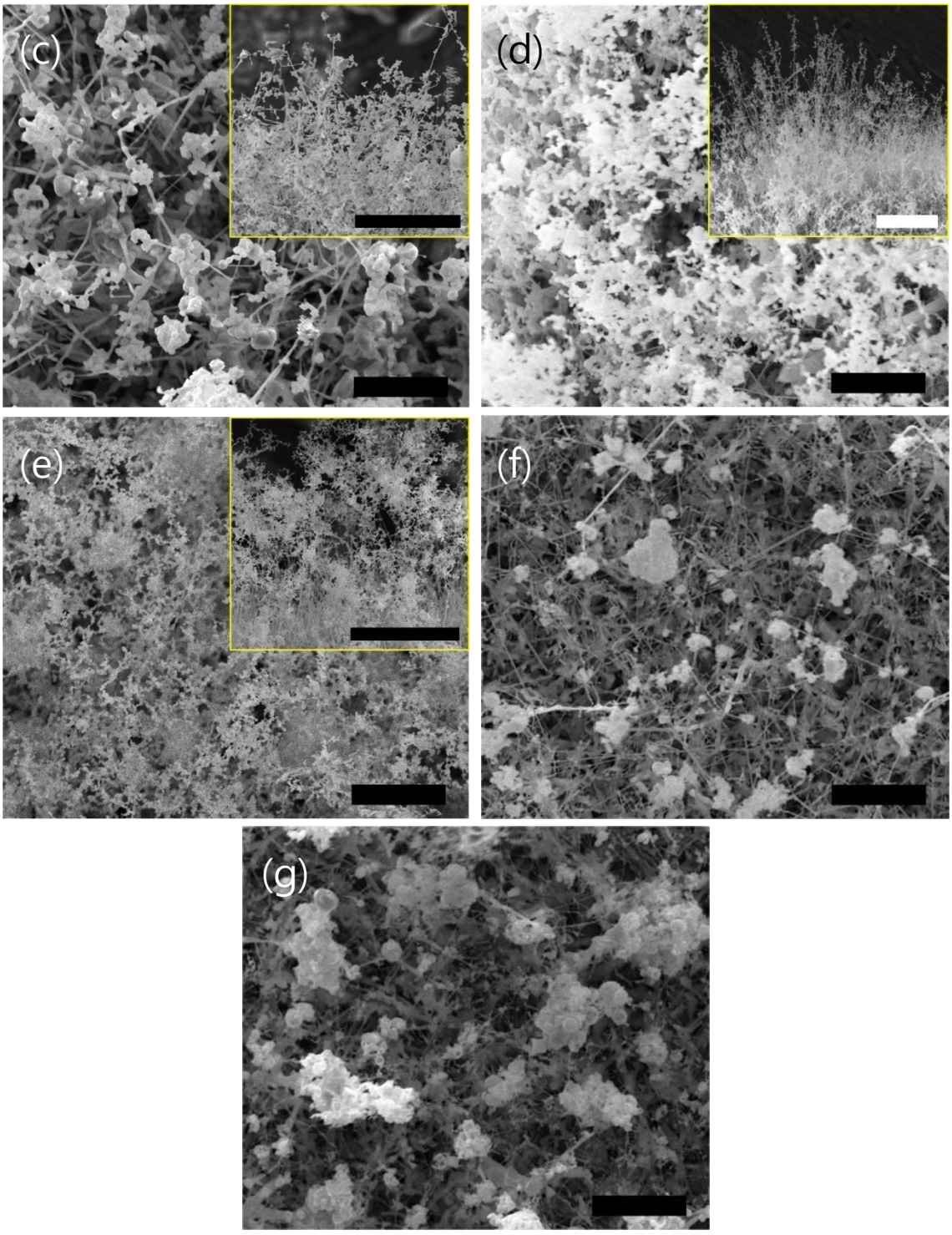

Figure 10. Continued.

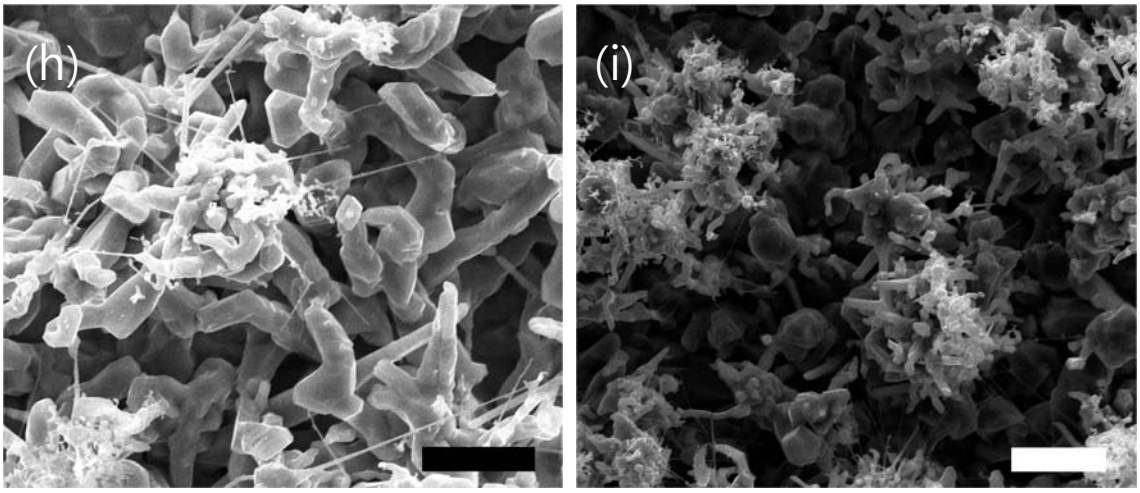

Figure 10. Continued.

3.2 Results and Discussion

TiO_2 nanowires were prepared according to the same procedure in Section 2.1 as shown in figure 10(a). The process of incorporating nanoparticles was carried out with the conditions as listed in table 2. TiO_2 hetero-structures were successfully obtained as shown in figures 10(d), (e) with the growth conditions 3, 4. The different reaction temperatures and the repetition times were studied by comparing the size of nanoparticles in figures 10(b), (c), (e) and (f), whose conditions were 1, 2, 4, and 5 respectively. The sample incorporated at 750 °C with repetition time of 20/20/20/20min showed the best result with smaller size of nanoparticles (~150 nm in diameter) and higher density than other temperatures.

Although the synthesis condition 1 showed successfully incorporated particle structures as shown in figure 10(b), the TiO_2 particles were grown to the micron scales

(~2 μm) due to the long repetition time of 60/30/30min. Furthermore, the repeated processes at a high reaction temperature affected the density of nanowires getting reduced and thickened. In order to examine the influence of the annealing temperature, only the parameter of the reaction temperature was changed to 750 °C (condition 2). However, the nanoparticle size was still large regardless of the reaction temperature (figure 10(c)). This result shows that the size of TiO_2 particles is more affected by the repetition time than the reaction temperature. Moreover, it observed that if there are not enough initial nanowires on the sample, nanoparticles could not be well-incorporated. This result explains that the nanowires grasp the $TiCl_4$ gas flows, and the $TiCl_4$ reacts with diffused oxygen to form nanoparticles. We also examined the effect of the repetition time in the process of nanoparticles growth. When the repetition time was changed to 20/20/20/20min, we can clearly see that shorter annealing time in each process reduces the sizes of nanoparticles as shown in the figures 10(d), (e).

The amount of Ti/ $CuCl_2 \cdot 2H_2O$ mixed powders was reduced to the half of the original amount (See condition 3 and 4) as each reaction time becomes shorter. We observed that there were no big changes according to the amount of mixed powders. The half amount of the mixed powders was fully enough to deliver $TiCl_4$ gases for incorporating nanoparticles on the nanowires structure as shown in figure 10(e).

For the further investigation of the temperature effect, the temperature of 650 °C was examined during the same repetition processes. By repeating the annealing processes, most powders reacted at this temperature as long as the temperature was much higher than the temperature that is fore-mentioned in chemical reaction formulas.

The nanoparticles, however, were not incorporated successfully. This result indicates that although the temperature of 650 °C saves the nanowires from the repeated annealing processes, the temperature is not enough to facilitate the reaction between nanowires and $TiCl_4$ vapors to synthesize TiO_2 nanoparticles as shown in figure 10(f). Therefore, the minimum annealing temperature (~ 750 °C) should be addressed to incorporate TiO_2 nanoparicles, although the annealing temperature is much higher than the temperature that is needed to activate the chemical reaction between Ti and $CuCl_2 \cdot 2H_2O$ powders.

As the same purpose, the ceramic boat was shifted 2.5 inches from the center to the downstream of the quartz tube to preserve the nanowires as much as possible from being destroyed by the repeated processes. By doing this, the site of the mixed powders is still placed on the active heating zone while the sample containing nanowires is located at the inactive heating zone. As a result, this act saved nanowires but caused the rapid nucleation of nanoparticle due to the sudden temperature drop. After all, the big size of particle or chuck was formed easily.

The simultaneous processes were studied, and the mixed powders were contained from the initial growth of nanowires in this method. The experiments were carried out at 750 °C and 850 °C with same repetition time (30/20/20/20min). The results showed that $TiCl_4$ vapors interrupted a growth of nanowire structures, and made it difficult for nanoparticles to be formed. Once more, this result explains that the initial nanowires structure should be formed before the incorporating process of nanoparticles.

From considering all the results, the condition of annealing 20/20/20/20min at 750 °C (condition 4) is the most suitable condition for incorporating TiO_2 nanoparticles while minimizing the destruction of nanowires.

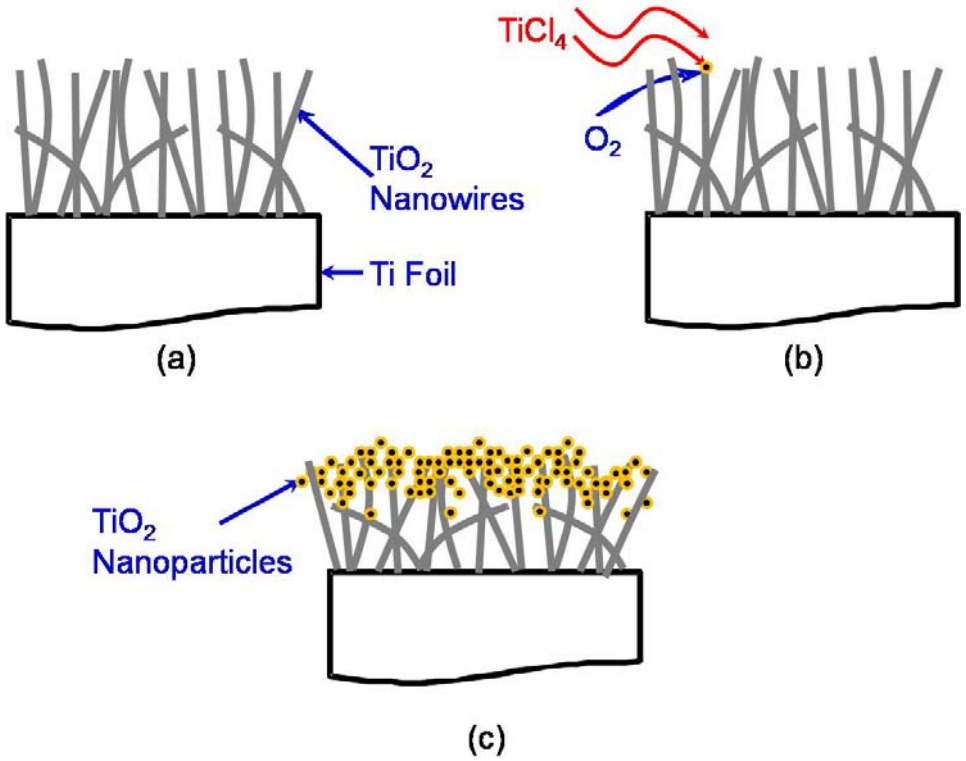

Figure 11. Proposed TiO_2 nanoparticles incorporation mechanism. (a) TiO_2 nanowires formed as a base structure. (b) Oxygen reacts with $TiCl_4$ vapors, producing crystalline TiO_2 nanoparticles. TiO_2 nanoparticles are naturally merged each other and with the nanowires at the elevated temperature. (c) Further reaction produces the groups of nanoparticles on the top side of the nanowires.

A proposed mechanism for this reaction is the following as shown in figure 11. First, the initial nanowires structure was formed as a base structure (figure 11(a)). Upon a heating process, the mixed powders of Ti and $CuCl_2 2H_2O$ bring $TiCl_4$ vapors to pass on the site of nanowires structure. At the same time, oxygen easily reacts to $TiCl_4$ vapors, producing crystalline TiO_2 nanoparticles. TiO_2 nanoparticles are naturally welded each other and sit on the nanowires structure at the elevated temperature (figure 11(b)). The repeated reactions with a relatively short annealing time produce the groups of nanoparticles on the top side of the nanowires (figure 11(c)).

In this experiment, oxygen was not supplied externally to the furnace tube during the reaction, but the oxygen is present from air residues and the Ar gas as impurity (oxygen in the 99.999% pure Ar gas is typically less than ~5 ppm) and/or TiO_2 nanowires on the Ti foils. This result suggests that an external supply of oxygen may not be necessary or should be avoided for incorporating TiO_2 nanoparticles.

To our best knowledge, such a vapor phase incorporation of TiO_2 nanoparticles by simply repeated thermal annealing method has not been reported elsewhere.

Figure 12 show bright field TEM images of nanoparticles with high resolution and two insets of diffraction patterns collected from the particles 1 and 2. Both particles are polycrystalline and the particle 2 displays twin boundaries. These results are fully natural since the nanoparticles were grown by repeated thermal annealing processes. The TEM images also show welded junctions between nanoparticles. This result might have occurred due to the direct incorporation at the relatively high reaction temperature. Two diffraction patterns were taken from the contact regions to see the orientation

relationship. They are indexed to have the rutile crystal structure while being aligned in the same 111 zone axis. The particles 1 and 2 are found to be oriented at the rotation angle of 48° with respect to each other. All these images and diffraction patterns clearly illustrate these nanoparticles grown under current synthesis condition are crystalline structures.

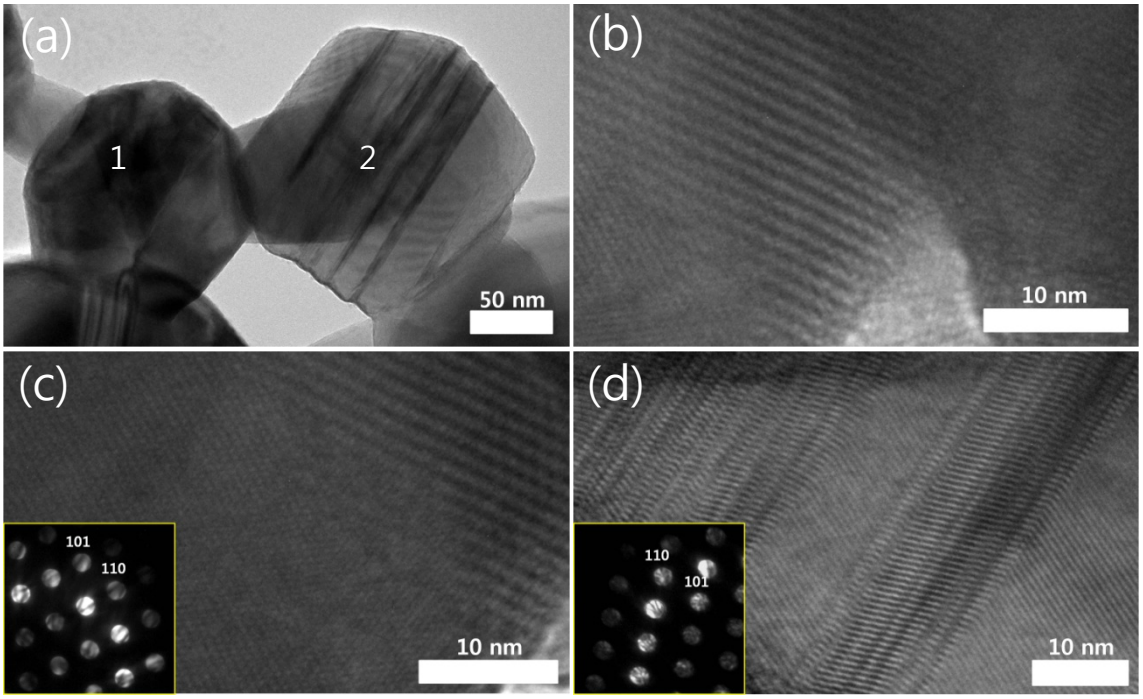

Figure 12. TEM images of nanoparticles. (a) a low magnification and (b) a high magnification at the junction of particle, (c) a high magnification of particle 1 with an inset of SAED pattern, and (d) a high magnification of particle 2 with an inset of SAED pattern. The sample was prepared at 750 °C with 20/20/20/20 minutes repetition times (condition 4).

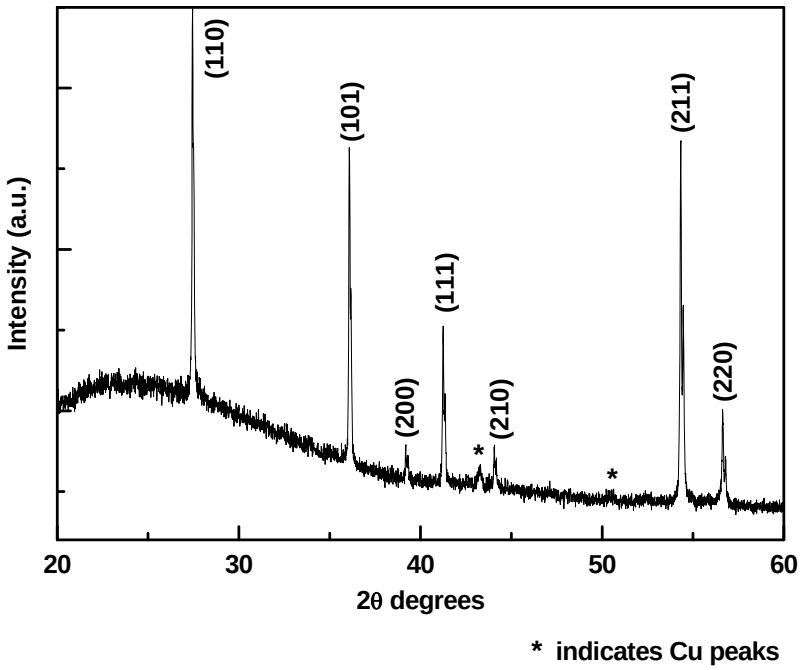

Figure 13. XRD pattern of TiO_2 hetero-structures. The nanoparticles were incorporated at 750 °C with 20/20/20/20 minutes repetition times (condition 4). This result indicates the TiO_2 hetero-structure is in the rutile structure. Crystal directions of the rutile structure TiO_2 are designated in the figure.

The TiO_2 hetero-structures were analyzed by XRD as shown in figure 13, XRD peaks indicate that the incorporated nanoparticles are also in the rutile structure the same as 1-D nanostructures, which is a common and stable form of TiO_2 [34, 35] synthesized at a temperature higher than ~600 °C [73, 74]. Chlorine-containing compounds such as $TiCl_2$, $TiCl_3$, $TiCl_4$, and $CuTiCl_4$ were not detected. Only small intensity peaks related

to Cu were observed. This was caused by the chance that Cu and/ or $CuCl_2$ were delivered to the sample as long as $CuCl_2 2H_2O$ were used as a catalyst to develop the $TiCl_4$ gases from the mixed powders.

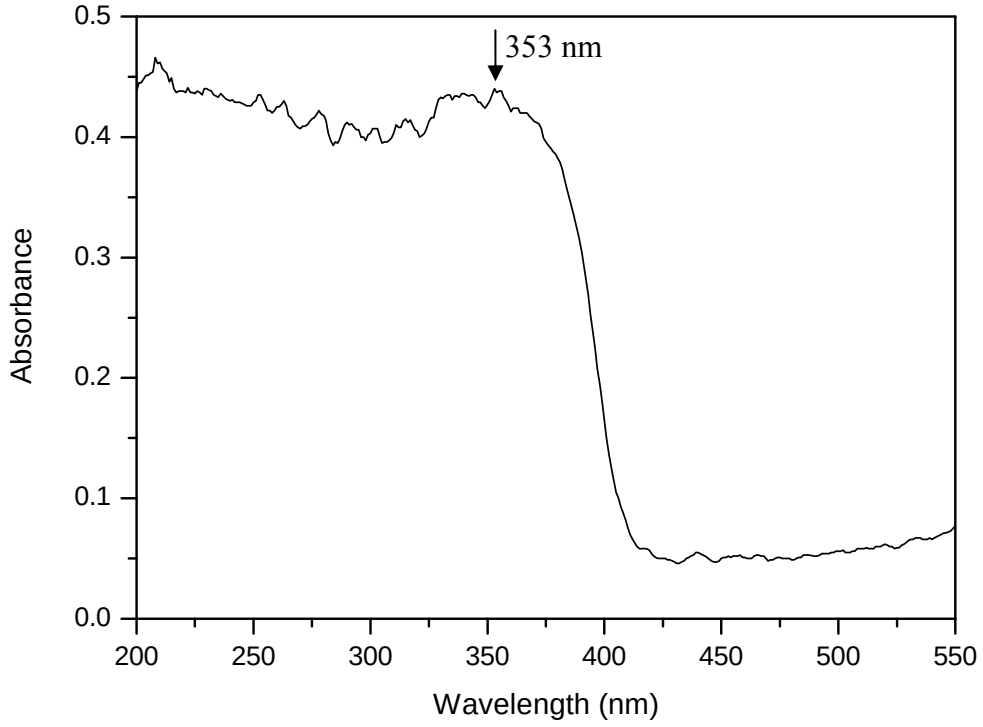

Figure 14. UV-visible light absorption spectra of TiO_2 hetero-structures.

In order to get more detail information, the sample was measured by using UV-visible light absorption spectroscopy (UV-vis). From this measurement, we may confirm that the Cu does not affect TiO_2 hetero-structure. Typically, bulk TiO_2 in a rutile

phase shows the light absorption peak at ~411nm, which corresponds to the band gap energy of 3.02 eV. However, TiO_2 hetero-structures show that the main absorption peak at 353 nm (3.52 eV) as shown in figure 14. This peak value is due to the quantum confinement effect of TiO_2 hetero-structures. Furthermore, this result also indicates that the structures do not contain any copper oxide related compounds, which have the smaller energy band gap (1.2 eV ~ 1.9eV) than TiO_2. Therefore, the Cu detected by XRD is nothing but just impurity that is spread on the surface of the sample.

4. CONCLUSIONS*

Single-crystalline one-dimensional rutile TiO_2 nanostructures were successfully synthesized from titanium foils by using a simple thermal annealing method at the atmospheric pressure. Moreover, TiO_2 nanoparticles were incorporated into 1-D nanostructures easily by using repeated thermal annealing processes. The synthesis method requires neither a high reaction temperature nor complicated reaction processes and can be used in producing dense nanowires and incorporating nanoparticles with relatively short reaction time. The key parameters of growing 1-D nanostructures are the eutectic catalyst, the reaction temperatures, and the annealing time. The reaction temperatures and the repetition time are important parameters for incorporating nanoparticles.

In brief, the Cu catalyst is essential to grow 1-D TiO_2 nanostructures at a temperature much lower than the melting point of Ti. The nanostructures were densely grown on the surface of foils with the use of Cu catalyst, but nanostructures were rarely seen on the samples synthesized without the catalyst. As a result, the reaction temperature close to the eutectic temperature of Ti and Cu is the most appropriate in growing nanostructures, and only 30 minutes of annealing time at 850 °C was enough to produce ~10 μm long and ~100 nm in diameter nanowires. Longer reaction time brought morphology changes from wires to belts as well as produced longer nanostructures up to ~30 μm. This morphology changes by the simple extension of the annealing time have not been reported elsewhere, but the change may be due to the

*Parts of this section reprinted with permission from "Simple and fast annealing synthesis of titanium dioxide nanostructures and morphology transformation during annealing processes" by Jongbok Park, Yeontack Ryu, Hansoo Kim, Choongho Yu, 2009, Nanotechnology, 20, 105608, Copyright [2009] by IOP.

preferential growth of rutile phase titania. The growth mechanism of 1-D TiO_2 nanostructures is thought to be solid-liquid-solid and/or solid/vapor-liquid/solid phase reactions, but it would be different from spontaneous whisker growth mechanisms.

The same chemical reaction formula was used to incorporate TiO_2 nanoparicles. Upon heating of Ti/ $CuCl_2 2H_2O$ mixed powders, $TiCl_4$ gases were developed according to a chemical reaction formula between CuCl and Ti. The created $TiCl_4$ gases were reacted with diffused oxygen to form TiO_2 nanoparticles on the nanowires structure. To activate this reaction, the minimum temperature of 750 °C or higher temperatures was needed. Moreover, the controlling of each annealing time in repeated processes affected on the size and the density of the nanoparticles. Consequently, the condition of 20/20/20/20min annealing at 750 °C was confirmed as the best condition for incorporating TiO_2 nanoparticles.

Further analysis using SEM, TEM, XRD, UV-vis was examined for the 1-D nanostructures and nanoparticles. Additionally, our simple and effective method for the synthesis of TiO_2 hetero-structures can be utilized for growing other types of metal oxide nanostructures especially for those whose melting temperatures are high.

5. FUTURE WORK

TiO_2 hetero-structures were successfully synthesized by using simple thermal annealing processes. These structures were grown at need to be utilized as an electrode in the dye-sensitized solar cells. Because of their structural characteristic, the DSSCs should be illuminated through the cathode side.

Figure 15 shows a proposed schematic diagram of backside illuminated DSSCs. Unlike the nanoparticle-based DSSCs, the titanium foil and the directly grown nanowires from the foil were used as the anode in the backside illuminated DSSCs. Normally, in the DSSCs made of TiO_2 nanoparticles, the anode side is deposited on the TCO so that the light can be absorbed directly from the front side. After all, the backside illuminated DSSCs have disadvantages, such as the light loss from Pt layer and electrolyte. Therefore, it is very crucial for backside illuminated DSSCs to maximize the transmittance. The thickness of Pt coating, the types of electrolyte, and the gap between the Ti foil and TCO will be key factors to reduce such disadvantages. However, there is a report that despite of these limitations, the backside illuminating system exhibits a larger open-circuit voltage compared to the front side illuminated DSSCs [27]. This result shows a potential for performance improvement in this type of DSSCs.

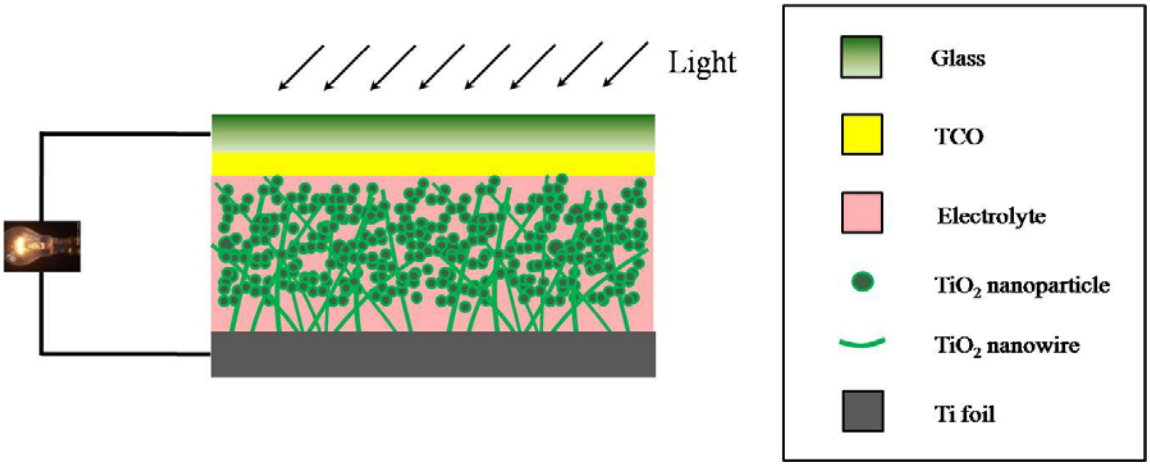

Figure 15. Proposed schematic diagram of backside illuminated dye-sensitized solar cells.

As a further step of this synthesis method, the direct growth method of hetero-structures on the TCO substrate can be suggested. By using this method, we can eliminate the disadvantages on backside illuminating system. Typically, ITO (idium tin oxide) or CNT thin film is used as a TCO substrate these days. ITO has a high melting point of ~1600 °C which is durable for the synthesis processes. Figure 16 depicts a proposed direct growth mechanism of TiO_2 hetero-structures on the TCO substrate. The Ti layers are deposited on top of the TCO by using a metal deposition (figure 16(b)). After that Cu is deposited on top of the Ti layer as a eutectic catalyst (figure 16(c)). By depositing Cu as a thin layer (~5 nm), the Ti-Cu eutectic reaction can be developed effectively, and this assists in a stable growth of TiO_2 nanowires. From this, the TiO_2 hetero-structures are synthesized according to the same procedure mentioned in previous

sections as shown in figure 16(d). Finally, transparent DSSCs on both sides are constructed, and the light can be absorbed through the front side (anode side) of DSSCs.

In order to achieve more efficient DSSCs from the TiO_2 hetero-structures, the further research should be studied. Especially, more detailed parameters such as the deposition thickness of each metal, the types of TCO substrates should be investigated for the successful direct growth method.

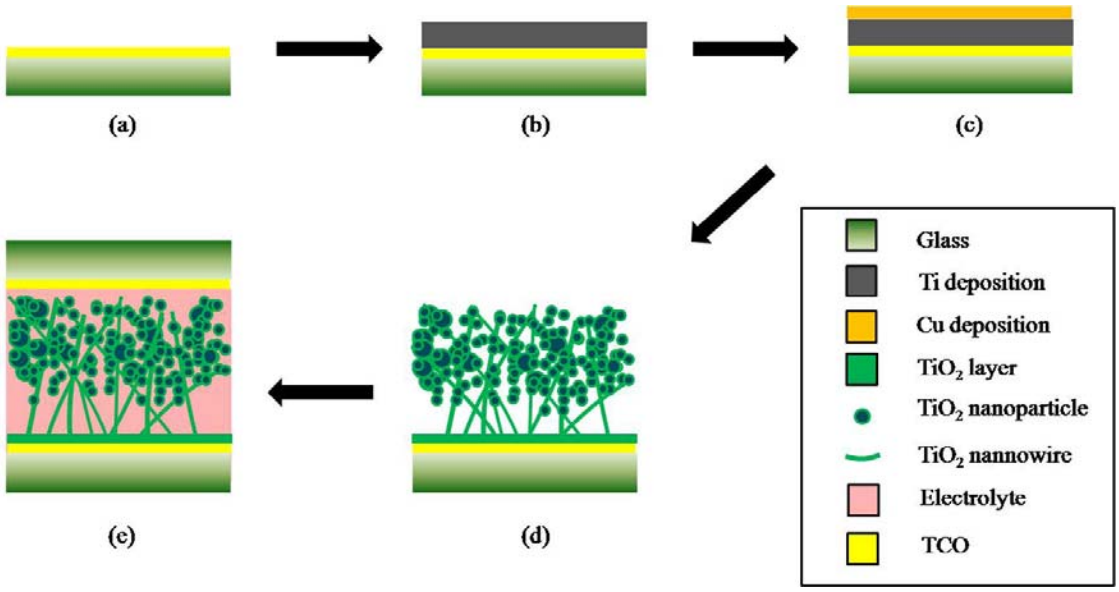

Figure 16. Proposed direct growth mechanism of TiO_2 hetero-structures on TCO substrate.

REFERENCES

[1] Li B, Wang L, Kang B, Wang P and Qiu Y 2006 *Sol. Energy Mater. Sol. Cells* **90** 549

[2] Gratzel M 2001 *Nature* **414** 338

[3] Chapin D M, Fuller C S and Pearson G L 1954 *J. Appl. Phys.* **25** 676

[4] Grant C D, Schwartzberg A M, Smestad G P, Kowalik J, Tolbert L M and Zhang J Z 2002 *J. Electroanal. Chem.* **522** 40

[5] Oregan B and Gratzel M 1991 *Nature* **353** 737

[6] Chiba Y, Islam A, Watanabe Y, Komiya R, Koide N and Han L Y 2006 *Jpn. J. Appl. Phys. Part 2 - Lett. Express Lett.* **45** L638

[7] Wang Q, Moser J E and Gratzel M 2005 *J. Phys. Chem. B* **109** 14945

[8] Podraza N J, Chi C, Sainju D, Ezekoye O, Horn M W, Wronski C R and Collins R W 2005 In: *Mater. Res. Soc. Symp. Proc.,* (Warrendale, PA: Materials Research Society) p 273

[9] Lee W J, Ramasamy E, Lee D Y, Min B K and Song J S 2006 In: *Proc. SPIE-Int. Soc. Opt. Eng.,* (Brisbane, Australia: SPIE) p 413

[10] Saito Y, Kambe S, Kitamura T, Wada Y and Yanagida S 2004 *Sol. Energy Mater. Sol. Cells* **83** 1

[11] Boercker J E, Enache-Pommer E and Aydil E S 2008 *Nanotechnology* **19** 095604

[12] Tan B and Wu Y Y 2006 *J. Phys. Chem. B* **110** 15932

[13] Feng X, Shankar K, Varghese O K, Paulose M, Latempa T J and Grimes C A 2008 *Nano Lett.* **8** 3781

[14] Wu J-J, Chen G-R, Lu C-C, Wu W-T and Chen J-S 2008 *Nanotechnology* **19** 105702

[15] Singh P, Kim K-I, Lee J-W and Rhee H-W 2006 *Phys. Status Solidi A* **203** R88

[16] Hara K, Nishikawa T, Kurashige M, Kawauchi H, Kashima T, Sayama K, Aika K and Arakawa H 2005 *Sol. Energy Mater. Sol. Cells* **85** 21

[17] Kusama H, Konishi Y, Sugihara H and Arakawa H 2003 *Sol. Energy Mater. Sol. Cells* **80** 167

[18] Pechy P, Renouard T, Zakeeruddin S M, Humphry-Baker R, Comte P, Liska P, Cevey L, Costa E, Shklover V, Spiccia L, Deacon G B, Bignozzi C A and Gratzel M 2001 *JACS* **123** 1613

[19] Nazeeruddin M K, Humphry-Baker R, Liska P and Gratzel M 2003 *J. Phys. Chem. B* **107** 8981

[20] Nakade S, Saito Y, Kubo W, Kitamura T, Wada Y and Yanagida S 2003 *J. Phys. Chem. B* **107** 8607

[21] Solbrand A, Lindstrom H, Rensmo H, Hagfeldt A, Lindquist S-E and Sodergren S 1997 *J. Phys. Chem. B* **101** 2514

[22] Fisher A C, Peter L M, Ponomarev E A, Walker A B and Wijayantha K G U 2000 *J. Phys. Chem. B* **104** 949

[23] van de Lagemaat J, Park N-G and Frank A J 2000 *J. Phys. Chem. B* **104** 2044

[24] Kopidakis N, Schiff E A, Park N-G, van de Lagemaat J and Frank A J 2000 *J. Phys. Chem. B* **104** 3930

[25] Kopidakis N, Neale N R, Zhu K, van de Lagemaat J and Frank A J 2005 *Appl. Phys. Lett.* **87** 202106

[26] Zhu K, Neale N R, Miedaner A and Frank A J 2007 *Nano Lett.* **7** 69

[27] Paulose M, Shankar K, Varghese O K, Mor G K, Hardin B and Grimes C A 2006 *Nanotechnology* **17** 1446

[28] Shankar K, Mor G K, Prakasam H E, Yoriya S, Paulose M, Varghese O K and Grimes C A 2007 *Nanotechnology* **18** 11

[29] Gratzel M 2004 *J. Photochem. Photobiol. A-Chem.* **164** 3

[30] Paulose M, Mor G K, Varghese O K, Shankar K and Grimes C A 2006 *J. Photochem. Photobiol. A-Chem.* **178** 8

[31] Wang Z L 2004 *Annu. Rev. Phys. Chem.* **55** 159

[32] Xia Y N, Yang P D, Sun Y G, Wu Y Y, Mayers B, Gates B, Yin Y D, Kim F and Yan Y Q 2003 *Adv. Mater.* **15** 353

[33] Chen X B and Mao S S 2006 *J. Nanosci. Nanotechnol.* **6** 906

[34] Wu J M, Wu W T and Shih H C 2005 *J. Electrochem. Soc.* **152** G613

[35] Daothong S, Songmee N, Thongtem S and Singjai P 2007 *Scr. Mater.* **57** 567

[36] Xiang B, Zhang Y, Wang Z, Luo X H, Zhu Y W, Zhang H Z and Yu D P 2005 *J. Phys. D: Appl. Phys.* **38** 1152

[37] Lei Y, Zhang L D, Meng G W, Li G H, Zhang X Y, Liang C H, Chen W and Wang S X 2001 *Appl. Phys. Lett.* **78** 1125

[38] Yoshida R, Suzuki Y and Yoshikawa S 2005 *J. Solid State Chem.* **178** 2179

[39] Wei M D, Konishi Y, Zhou H S, Sugihara H and Arakawa H 2004 *Chem. Phys. Lett.* **400** 231

[40] Francioso L and Siciliano P 2006 *Nanotechnology* **17** 3761

[41] Li A P, Muller F, Birner A, Nielsch K and Gosele U 1999 *Adv. Mater.* **11** 483

[42] Lee W, Ji R, Gosele U and Nielsch K 2006 *Nat. Mater.* **5** 741

[43] Masuda H, Yamada H, Satoh M, Asoh H, Nakao M and Tamamura T 1997 *Appl. Phys. Lett.* **71** 2770

[44] Dang H Y, Wang J and Fan S S 2003 *Nanotechnology* **14** 738

[45] Pan Z W, Dai Z R and Wang Z L 2001 *Science* **291** 1947

[46] Saunders N 1985 *Calphad* **9** 297

[47] Chase M W 1998 *NIST-JANAF Thermochemical Tables* (Washington, DC: American Chemical Society)

[48] Gillot B, Souha H and Radid M 1992 *J. Alloy. Compd.* **184** 211

[49] Gillot B, Radid M, Sbai K and Souha H 1998 *J. Alloy. Compd.* **274** 90

[50] Yu T, Zhu Y W, Xu X J, Yeong K S, Shen Z X, Chen P, Lim C T, Thong J T L and Sow C H 2006 *Small* **2** 80

[51] Zhang K, Rossi C, Tenailleau C, Alphonse P and Chane-Ching J 2007 *Nanotechnology* **18** 8

[52] Fu Y Y, Wang R M, Xu J, Chen J, Yan Y, Narlikar A and Zhang H 2003 *Chem. Phys. Lett.* **379** 373

[53] Wagner R S and Ellis W C 1964 *Appl. Phys. Lett.* **4** 89

[54] Zhang Y J, Wang N L, He R R, Liu J, Zhang X Z and Zhu J 2001 *J. Cryst. Growth* **233** 803

[55] Chih-Yuan W, Lih-Hsiung C, Da-Qing X, Tien-Chih L and Han C S 2006 *J. Vac. Sci. Technol., B* **24** 613

[56] Kim C H, Chun H J, Kim D S, Kim S Y, Park J, Moon J Y, Lee G, Yoon J, Jo Y, Jung M H, Jung S I and Lee C J 2006 *Appl. Phys. Lett.* **89** 223103

[57] Jiang X C, Herricks T and Xia Y N 2002 *Nano Lett.* **2** 1333

[58] Fu Y Y, Chen J and Zhang H 2001 *Chem. Phys. Lett.* **350** 491

[59] Wang R M, Chen Y F, Fu Y Y, Zhang H and Kisielowski C 2005 *J. Phys. Chem. B* **109** 12245

[60] Xu Y Y, Rui X F, Fu Y Y and Zhang H 2005 *Chem. Phys. Lett.* **410** 36

[61] Wen X G, Wang S H, Ding Y, Wang Z L and Yang S H 2005 *J. Phys. Chem. B* **109** 215

[62] Fan Z Y, Wen X G, Yang S H and Lu J G 2005 *Appl. Phys. Lett.* **87** 013113

[63] Zhu Y W, Yu T, Sow C H, Liu Y J, Wee A T S, Xu X J, Lim C T and Thong J T L 2005 *Appl. Phys. Lett.* **87** 023103

[64] Yan Y G, Zhou L X, Zhang J, Zeng H B, Zhang Y and Zhang L D 2008 *J. Phys. Chem. C* **112** 10412

[65] Dai Z R, Pan Z W and Wang Z L 2001 *Solid State Commun.* **118** 351

[66] Fang X S, Ye C H, Peng X S, Wang Y H, Wu Y C and Zhang L D 2003 *J. Mater. Chem.* **13** 3040

[67] Wang Z L 2003 *Adv. Mater.* **15** 432

[68] Lee J C, Park K S, Kim T G, Choi H J and Sung Y M 2006 *Nanotechnology* **17** 4317

[69] Yang H G and Zeng H C 2005 *J. Am. Chem. Soc.* **127** 270

[70] Bavykin D V, Friedrich J M and Walsh F C 2006 *Adv. Mater.* **18** 2807

[71] Lin Y, Wu G S, Yuan X Y, Xie T and Zhang L D 2003 *J. Phys.-Condes. Matter* **15** 2917

[72] Liu S Q and Huang K L 2005 *Sol. Energy Mater. Sol. Cells* **85** 125

[73] Ouyang M, Bai R, Yang L, Chen Q, Han Y, Wang M, Yang Y and Chen H 2008 *J. Phys. Chem. C* **112** 2343

[74] Dachille F, Simons P Y and Roy R 1968 *Am. Miner.* **53** 1929

VITA

Jongbok Park received his Bachelor of Science degree in mechanical engineering from Korea Military Academy at South Korea in 2004. He entered the Mechanical Engineering program at Texas A&M University in September 2007 and received his Master of Science degree in August 2009. His research interests include synthesis of 1-D metal oxide nanostructures and photovoltaic energy conversion applications. He plans to adapt his research topics to the power sources of the electric equipments in the military.

Cpt. Park may be reached at Nano-Energy Laboratory, 403 Engineering/Physics Building (ENPH), Department of Mechanical Engineering, Texas A&M University, College Station, TX 77843-3123. His email is jbpark64@gmail.com.